# Tectonic Setting, Structure, and Seismic Stratigraphy of the Apalachicola Rift and its Overlying Sag Basin in the Northeastern Gulf of Mexico

by
Matthew Luis Storey

A thesis submitted to the faculty of the Department of Earth and Atmospheric Sciences,
College of Natural Sciences and Mathematics
in partial fulfillment of the requirements for the degree of

MASTER OF SCIENCE

in Geophysics

Chair of Committee: Dr. Paul Mann

Committee Member: Dr. Jonny Wu

Committee Member: Ted Godo

University of Houston
May 2020

# ACKNOWLEDGMENTS

I thank my thesis supervisor, Dr. Paul Mann, for his guidance and support throughout my final year of the master's program at the University of Houston. I have learned a great deal from him both about geology and the value of hard work during this last year of graduate school. I am extremely grateful for the many opportunities that Dr. Mann and the CBTH consortium have provided me. I am thankful for the company sponsors of the Conjugate Basins, Tectonics, and Hydrocarbons (CBTH) consortium that have provided my financial support as a graduate research assistant. Some of my best experiences during graduate school are related to my experiences with the CBTH group that were only made possible by their financial support.

I also thank Dr. Jonny Wu for his service on my thesis committee and valuable input, along with Ted Godo for sharing his vast experience and guiding my understanding of the Gulf of Mexico. Finally, I thank Mike Saunders at Spectrum Geo (now TGS) for providing the seismic data set that was used in the study.

I would like to thank the many friends I have made in the CBTH group and in UH graduate courses along with my interactions with the many academic researchers and industry professionals I have met at CBTH meetings and conferences. It has truly been a fun and life-changing ride and I am extremely grateful for each second of the graduate experience. Finally, I want to thank my family for their love and continuous support.

# ABSTRACT

The northeast-trending Apalachicola rift (AR) in the northeastern Gulf of Mexico (GOM) is a ~220-km- long half-graben that contains 5-8 km of undrilled, syn-rift clastic deposits inferred to be of late Triassic-early Jurassic age. Previous workers have interpreted pre-salt (Triassic-early Jurassic), basinward-dipping, seismic reflectors within the syn-rift half-graben of the AR as either: 1) volcanic layers or sills erupted and tilted within Mesozoic half-grabens; or 2) as layered, volcanic flows ("seaward-dipping reflectors") erupted during GOM phase 1 rifting of late Triassic- early Jurassic age.

My study uses a 35,000 km grid of 2D, pre-stack depth-migrated, industry seismic reflection data, tied to five wells in the overlying sag basin to map these enigmatic reflectors in three dimensions to distinguish these two previous interpretations and to improve structural and stratigraphic interpretations of the syn-rift and sag phases of the AR. Mapping of a seismic grid reveals that the AR is a composite rift composed of two major *en echelon* half-grabens: 1) a 136-km-long, northwest-trending half-graben with dips around 33° to the northeast; and 2) a 75-km-long, northwest-trending half-graben normal fault with dips around 31° to the northeast. Both half-grabens contain basinward-dipping reflectors with observable stratigraphic wedging controlled by the dips of low-angle normal faults (LANFs). The observed dip range of bounding normal faults is consistent with previous work on rift-related LANFs in the northeastern GOM and along the eastern coast of North America.

Mapping of the seismic grid shows a similar Phase 1 rift, called the Elbow rift, which is located 200 km to the southeast of the AR. Together the AR and Elbow rift form a 300-km long and a 40-km wide belt of rifting that crosscuts the northwest-trending Paleozoic orogenic and

earlier rift fabric beneath the West Florida shelf and the mainland of Florida. I interpret the parallelism of the AR-Elbow rift trend with the marginal rifts bordering oceanic crust ~200 km to the southwest as indicating that both sets of rifts are part of the second phase of rifting in GOM that was related to the late Jurassic, counterclockwise rotation of the Yucatan block.

# LIST OF FIGURES

boundary between pre-rift sediments and basement is interpreted based on these findings.

**Figure 5.** Locations of seismic lines and well data used for this study are shown on a bathymetric basemap. The Deep East seismic reflection survey was provided by Spectrum (now TGS) and consists of a ~35,000 line km 2D PSDM reflection survey with depth penetrations down to the Moho (~30-40 km). 15 lines are used from that survey to investigate rifting beneath the Apalachicola basin. The seismic lines labeled with figure numbers appear in this study. Six wells in the overlying Apalachicola post-rift sag were used to correlate stratigraphy beneath the top Louann salt. Nearby wells in the Tampa Embayment and from published papers (Hunter, 2014; Godo, 2017; Lin, 2018) were used to correlate Mesozoic and Cenozoic units across the West Florida Shelf. The Sohio (GV-707) and Sake #2 (DC) are used as offshore Triassic sediment analogs for the Apalachicola pre-salt sediments. Wells further to the southeast mostly constitute basement penetrations and can be found described in Christenson (1990). Black faults represent half-graben normal faults from this study. Gray faults represent extensional post-rift salt tectonics from Pashin et al. (2016). **SGR**=South Georgia Rift, **BFZ**=Bahamas Fracture Zone, **COB**=Continent-Ocean Boundary, and **MOR**=Mid-Ocean Ridge.

**Figure 6.** Generalized stratigraphy for the EGOM modified from Lin (2018). No well penetrates beneath the Louann Salt in the Apalachicola area, therefore, the Apalachicola syn-rift section (Eagle Mills Formation) is inferred only from seismic reflection data. Following Louann Salt deposition was Phase 2 rifting which included Jurassic units such as the Norphlet, Smackover, Haynesville, and Cotton-Valley formations. Following the Jurassic deposition was a thick (~5 km) sequence of Cretaceous passive margin carbonate-clastic sedimentation.

**Figure 7**. **A.** Uninterpreted northeast-trending seismic line DE-1699 across the Apalachicola basin and rift. Location of seismic line shown on map in Figure 5. **B.** Interpreted northeast-trending seismic line that illustrates the post-rift stratigraphy in the Apalachicola basin. The sag basin is characterized by a relatively thin (~3 km) sequence of Jurassic sediments overlain by a thicker (~5 km) Cretaceous sequence. Salt tectonics controls many potential hydrocarbon traps as shown by salt withdrawal up-dip into domal structures which creates a zone of thickening in the overlying Cretaceous section in the center of the sag. Salt rollers, salt pillows, and diapirs are also prevalent throughout the basin. The southwest-dipping normal fault on the northeast-side of the line represents the up-dip limit of salt tectonics due to gravity sliding and sediment loading that rims around the peripheral of the Apalachicola basin and is known as the Destin fault system (Pashin et al., 2016). Moving southwest away from the interpreted half-graben, there is little evidence for faults or tilted fault blocks as the crust there largely represents the southernmost extent of the Southern Platform.

**Figure 8.** Structure maps for the Callovian, Oxfordian, Kimmeridgian, and Tithonian periods in the area of the early Phase 1 Apalachicola rift illustrating sediment fill in the basin. **A.** Mid-Jurassic unconformity. This map represents the period time immediately after Phase

1 rifting and is evident as a relatively smooth erosional unconformity that is mappable along the west Florida Shelf. **B.** Top Oxfordian. Marks the top of the Smackover carbonates and Norphlet sandstone formations that lie above the Louann Salt and together represent the early stages of basin fill in this area. **C.** Top Kimmeridgian. Deposition of the Haynesville formation which primarily includes sandstone fill on the shelf and shale towards the GOM basin. **D.** Top Tithonian. Represents the base of the Cretaceous section and includes the deposition of Cotton-Valley formation which consists primarily of sandstone in the basin. The overlying post-rift has an east-west trend and contains deeper sections seaward. **E.** The base syn-rift map shows a northwest orientation which parallels the shallow Moho/gravity trend under the rift as shown in Figure 1. **F.** An isopach between the Base Syn-rift and mid-Jurassic unconformity surfaces reveals up to around 6-7 km of syn-rift thickness in these rifts. Seismic observations show thicknesses up to 10 km depending on the exact depth of the syn-rift/pre-rift boundary.

**Figure 9. A.** Uninterpreted northeast-trending seismic dip-line DE-1643 across the Apalachicola rift. Location of seismic line shown on map in Figure 5. **B.** Interpreted northeast-trending seismic dip-line illustrating a low-angle half-graben normal fault. The normal fault dips around 33° to the northeast and is likely detaching into weaker crust around 20-22 km in depth. This fault dip is consistent with low-angle normal fault basins along the east coast such as the Newark Basin that dips at 30° and is the reactivation of Paleozoic thrust features in the Appalachian region (Withjack et al., 2013). Deeper stratigraphic units have a gentle dip around 16° with younger units having progressively shallower dips. Pre-rift and/or basement reflectors appear to truncate along the approximate syn-rift base. An approximate pre-rift zone of Paleozoic clastics/metasedimentary is interpreted based on the nearby FM-252 well that drilled into Orodovician clastics without encountering igneous basement.

**Figure 10. A.** Uninterpreted northwest-trending seismic strike line DE-380a and DE-380b in northern section of the Apalachicola rift. Location of seismic line shown on map in Figure 5. **B.** Interpreted northwest-trending seismic strike line that includes the seismic displayed in Figure 4. This figure illustrates intrabasin highs and lows of unlinked half-graben normal faults that create undulating ramps. A similar example from a low-angle fault system occurs in Thailand as seen in Figure 11 from Morley (2009).

**Figure 11. A.** Uninterpreted north-trending seismic dip-line DE-533 across the Apalachicola rift. Location of seismic line shown on map in Figure 5. **B.** Interpreted northeast-trending seismic dip-line illustrating a half-graben normal fault dipping 31° to the northeast and with a detachment possibly around 24 km in depth. Deeper interpreted horizons have high dips around 28°-40° indicating significant rotation involved in the rifting process. Fold-like reflections are interpreted towards the north and likely represent Paleozoic compressional features that provide the initial structural weaknesses required to produce low-angle faults.

**Figure 12. A.** Uninterpreted northwest-trending seismic strike line DE-377 across the center of

the Apalachicola basin. Location of seismic line shown on map in Figure 5. **B.** Interpreted northwest-trending seismic strike that illustrates typical strike view of a half-graben with bowl-shaped geometries, northwest-dipping, and southeast-dipping reflections, overlying sag, and onlapping reflections. **C.** Schematic map view of a half-graben with uplifted and down-thrown blocks with seismic transects indicated. **D.** Schematic transverse or dip view A-A' across the fault illustrating the expected half-graben geometry. Sediment is thickening towards the boundary fault and progressively thinning and onlapping towards the flexed margin. **E.** Schematic longitudinal or strike view illustrating the bowl-shaped unfaulted basin with sediment thickest in the center near maximum fault displacement and progressively thinning towards the margins. Figures **C-D** are modified from Withjack et al. (2002).

**Figure 13. A.** Structural modeling of the seismic profile shown in Figure 9 reveals a needed fault dip angle of 32.7° and a detachment around 20 km in depth to restore interpreted horizons with the equivalent modeled structural surfaces. Erosion of around 2-3 km is likely to have taken place based upon stratigraphic syn-rift truncations along the Middle Jurassic unconformity. This unconformity appears as a relatively smooth angular unconformity across the West Florida Shelf and indicates that significant erosion of presalt strata took place over a long period (MacRae and Watkins, 1995). The amount of erosion is also consistent with erosion estimates calculated from vitrinite reflectance data in the Newark Basin (Withjack et al., 2013). **B.** Forward modeling of the half-graben structural evolution is based on conventional ages associated with Phase 1 rifting (late Triassic-early Jurassic). Based on the inferred ages, erosion is modeled to begin around 175 Ma at a rate of 342 m/Myr. Rifting likely ended much sooner and was followed by continued presalt deposition based on planar-like stratigraphic units that truncate against the unconformity and are identified as graben spill-over.

**Figure 14. A.** Uninterpreted northeast-trending seismic line DE-630 crossing the Elbow rift on the northeastern edge of the Tampa Embayment. Location of seismic line shown on map in Figure 5. **B.** Interpreted northeast-trending seismic line that illustrates a rift that is parallel with the Apalachicola rift trend and perpendicular to northeastern Paleozoic orogenic activity. During Phase 1 rifting, this syncline likely experienced extensional forces resulted in accomodation space for Triassic sedimentation to occur. **C.** Uninterpreted north-south trending seismic line DE-554 across the Apalachicola rift. Location of seismic line shown on map in Figure 5. **D.** Interpreted north-south trending seismic line illustrating a half-graben adjacent to a syncline. Arden (1974) observed synclines in onshore Florida near the Apalachicola embayment and interpreted them as Paleozoic in origin and containing Silurian to Devonian sediments.

**Figure 15. A.** Uninterpreted northwest-trending seismic line DE-436 and DE-438 crossing the Sohio GV-707 well. Location of seismic line shown on map in Figure 5. **B.** Interpreted northwest-trending seismic profiles illustrating Triassic syn-rift deposits and a possible graben filled with Triassic-Paleozoic sediments. **C.** Interpreted log from the bottom interval of the Sohio well that penetrated up to 2 km of sediment and igneous material.

**Figure 16.** Seismic facies classification using seismic character analysis as described by Bally (1987). Location of seismic lines shown on map in Figure 5. Eight features from the syn-rift from lines DE-1643, DE-1595, and DE-1699 are described using seismic character traits such as reflection configuration, continuity, amplitude, and frequency to determine the possible environment of deposition. Except for the inferred coarse-grained, fault-scarp breccias shown as SF-8, the other seismic facies 1-7 shown are well layered and indicative of a finer-grained, fluvial or submarine syn-rift deposit. The observed variability in fault wedging is inferred to reflect variations in the amount of fault activity during their deposition.

**Figure 17.** Inferred seismic stratigraphic facies based on typical continental rift deposits from Burg (2018), Davison and Underhill (2012) and from nearby well penetrations such as Sake #2 Frederick et al. (2016), the Sohio GV-707 well, and in the TX-Lou-Ark region. Along the boundary fault, coarse deposits of erosional fill from the uplifted footwall are expected and can be seen as chaotic reflectors and alluvial fans coming off the fault. The syn-rift contains noticeable bright amplitude diverging reflections likely representing an early rift phase that is fluvial dominated with sandstones and red-green oxic shales and volcaniclastics. The mid-rift to late-rift phase contains alluvial fans and channels near the boundary fault, and a thick section of low amplitude reflections indicating a homogenous layer likely of red bed origin. After rifting, continued deposition is evident in form of planar onlapping and truncated reflections thus likely representing an early sag phase that is fluvial dominated with sandstones, siltstones, and shale. Inferred basalt dikes and sills are included based on the abundance of well records encountering Eagle Mills deposits containing intrusion and volcaniclastic sediments dated as young as early Jurassic.

**Figure 18. A.** Merged Bouguer gravity map modified from Bain et al. (2019) for the eastern GOM. This figure illustrates the gravity high trend for early Phase 2 rifts shown in white, later Phase 2 rifts adjacent to the oceanic crust in the deep GOM in white, and the continent-ocean boundary in yellow from Nguyen and Mann (2016). The eastwest to southeast trend of the early Phase 1 Apalachicola rift and Elbow rift is orthogonal to and crosscuts the older, northeast-trending Phase 1 trend and Paleozoic orogeny trend beneath Florida and the West Florida Shelf. The trend of the Florida Lineament (Fig. 2) shown as the zone between the dashed yellow lines forms the approximate boundary between the northeast Phase 1-orogenic trend and the younger Phase 2 trend of the Apalachicola and Elbow rifts. **B.** Total magnetic intensity anomaly for the EGOM from Lin (2018) that further illustrates the crosscutting trend of the early Phase 1 Apalachicola and Elbow rifts. Both rifts are represented by the elongate trends of magnetic highs. The Tampa Embayment exhibits a ~40-km, left-lateral offset from the older Paleozoic Suwannee Basin in the north as defined by a prominent magnetic low and illustrated by white-distance markers around the 6 km mark.

**Figure. 19.** Plate reconstruction for the Gulf of Mexico modified from (Lin, 2018). **A.** The late Paleozoic collision resulting in the formation of Pangea, ending in the Permian. **B.**

Initiation of Phase 1 GOM rifting during the late Triassic to early Jurassic. **C.** By the end of Phase 1 rifting, many northeast-trending faults are opened as well as the early Phase 2 Apalachicola Rift which cross-cuts the onshore older northeast-trending rifts. Additionally, the proposed north-northwest onshore continuation of the rift is projected and connecting with the Texas-Louisiana-Arkansas basin. **D.** Salt deposition begins in the middle Jurassic. **E.** Phase 2 GOM rifting and oceanic spreading occurs followed by counterclockwise rotation of the Yucatan block. **F.** Phase 2 rifting, spreading, and rotating ends in the early Cretaceous

# CHAPTER 1: INTRODUCTION TO THIS THESIS

## 1.1 History and development of this thesis

My interest in geology began at an early age as I enjoyed exploring nature at every opportunity. San Antonio, Texas, is an excellent place to explore and it was there that I found my first fossil, a large, Cretaceous gastropod the size of my hand. I accumulated containers of fossils, minerals, and sedimentary and igneous rocks that I have collected from my childhood and continued through my later travels around the world. These early experiences led to my majoring in geology and mathematics and graduation with a 2017 BSc degree in Geophysics from Texas A&M University.

Following my graduation, I began a fulltime job as a geo-tech for a geophysical consulting company in Corpus Christi, Texas, and gained my first experience in subsurface, seismic mapping. During this time, I decided to pursue a master's degree and ended up enrolling as a non-thesis student in geophysics at University of Houston during the fall semester of 2018.

After one year in graduate school, I was accepted as a master's thesis student by Dr. Paul Mann, a professor and principal investigator of the Conjugate Basins, Tectonics, and Hydrocarbons (CBTH) research consortium at the University of Houston. I had previously taken both the Basin Analysis course in the fall of 2018 and the Petroleum Prospecting course in the spring of 2019 that were both taught by Dr. Mann.

My master's project with the CBTH project focused on the pre-salt rifting architecture in the Apalachicola Basin of the offshore northeastern Gulf of Mexico that is described in detail in this thesis. Previous CBTH students who had investigated this same area of the northeastern

GOM included Mei Liu (Liu et al., 2019) and Pin Lin (Lin, 2018) who had contributed results from gravity/magnetic modeling and detailed seismic mapping using some of the same Spectrum (now TGS data) that I have used in this master's thesis. However, some questions remained for the evolution of the northeast GOM such as the relationship between rifting in the Apalachicola region to rifting onshore in Florida - as well as the general timing of these Apalachicola rifts in relation to conventional ages associated with the GOM opening. As I started to read previous publications on this area, I began to focus on questions concerning the petroleum potential of pre-salt sediments, the paleogeography during pre-Jurassic times, and the lack of seismic evidence of extensive Phase 1 rifting in the Gulf of Mexico. My external committee member, Ted Godo, provided me with an extensive set of readings on the northeastern GOM that included his own research in the area during his 35 years with Shell and Murphy Oil (Godo, 2017).

Dr. Mann and the CBTH project had a longterm working relationship with one of the CBTH sponsors, Spectrum Geo (now TGS), that allowed us to reach out to Mike Saunders at Spectrum Geo for access to their Deep East seismic survey. I was allowed access to the recently reprocessed 2D PSDM data and began my master's study in June of 2019. I spent the summer of 2019 working at the Spectrum Geo office and completing mapping of the Deep East seismic grid in my area. The depth penetration and quality of the Deep East seismic grid allowed me to investigate the pre-salt stratigraphy of the Apalachicola area which was not possible from the seismic data available to the previous generation of geoscientists who had worked in this same area (Dobson and Buffler, 1991; MacRae and Watkins, 1995).

Although my time as a member of the CBTH project has been less than one year, the fast-paced work environment of the CBTH group provided me the opportunity to present at two

conferences as well as giving 6 presentations to CBTH sponsors. These conferences included the 2019 Houston Geological Society-University of Houston Sheriff Lecture in Houston (Storey and Mann, 2019), and the 2020 AAPG Hedberg Conference on pre-salt stratigraphy in Mexico City, Mexico (Storey and Mann, 2020) for which I was an invited as a graduate student presenter. The feedback I received at both conferences was important for developing the conclusions presented in this thesis and am thankful for the meeting organizers and the many experts who took the time to examine and critique my work.

This thesis summarizes the main conclusions of my seismic mapping in the Apalachicola Basin and along the West Florida Shelf. Specific topics that I address include: 1) better definition of the late Jurassic-Cenozoic sag basin stratigraphy that overlies the Louann salt; 2) improved mapping and seismic imaging of the listric normal fault geometry that controls the pre-salt, syn-rift section; 3) improved mapping to better define the orientation of rifting in the Apalachicola area in order to relate it to the Phase 2 rifting event in the GOM; and 4) improved inferences on the nature of the pre-salt, syn-rift stratigraphy based on a more detailed summary of seismic facies.

# CHAPTER 2: TECTONIC SETTING, STRUCTURE, AND SEISMIC STRATIGRAPHY OF THE APALACHICOLA RIFT AND ITS OVERLYING SAG BASIN IN THE NORTHEASTERN GULF OF MEXICO

## 2.1 Introduction

### 2.1.1 Significance of GOM opening phases

The Gulf of Mexico (GOM) basin opening and formation involves a two-phase history of rifting and oceanic crust emplacement that spans the late Triassic to early Cretaceous (Eddy et al., 2014; Hudec and Norton, 2019; Steier and Mann, 2019) (Fig. 1A, B). Eddy et al. (2014) first proposed that Phase 1 GOM opening was oriented in a northwest-southeast extensional direction that initiated during the late Triassic-early Jurassic separation of the North and South American plates. This Phase 1 GOM event was colinear with the much better studied, northeast-southwest-trending rifts that are present along the eastern margin of North America (ENAM) (Olsen, 1990; Withjack et al., 2013) (Fig. 1A, B).

After a brief Callovian sag phase in the GOM during which the massive Louann-Campeche salt body was deposited above the subsiding, late Triassic-early Jurassic, Phase 1 rifts, late Jurassic, Phase 2 rifting accompanied rotation of the Yucatán block by 37°-40° in a counterclockwise direction. This counter-clockwise rotation of the Yucatan block led to the formation of oceanic crust that was emplaced during the late Jurassic to earliest Cretaceous (Steier and Mann, 2019; Liu et al., 2019). This younger Phase 2 extension produced eastwest-trending marginal rifts that formed directly adjacent to the newly formed oceanic

crust in the central GOM (Nguyen and Mann, 2016; Steier and Mann, 2019; Liu et al., 2019) (Fig. 1A, B).

**Figure 1. A.** Regional gravity inversion of GOM, Southern USA, and Mexico by Liu (personal communication, 2020). This figure displays crustal thickness variations across the GOM region. Depth to basement contours (km) modified from Sawyer et al. (1991) and Ewing and Galloway (2019). Red to pink zones indicate thick continental crust (> 40 km). Green zones indicate thick transitional to transitional crust (20-30 km). Blue zones indicate thin crust/oceanic crust (4-12 km). Black faults represent Phase 1 and Phase 2 rifting. northeast-trending faults correspond to Phase 1 and faults along the COB represent Phase 2. **B.** Zoom on EGOM West Florida Shelf. White dots indicate interpreted Moho picks from my seismic data grid. Black dashed outlines indicate zones of rift-related, crustal thinning. **AR**=Apalachicola Rift, **ER**=Elbow Rift, **WA**=Wiggins Arch, **MOR**=Mid Ocean Ridge, **COB**=Continent-Oceanic Boundary, **SGR**=South Georgia Rift, **AOB**=Appalachian Orogenic Belt, **TE**=Tampa Embayment, **SA**=Sarasota Arch, **MGA**=Middle Ground Arch, **SP**= Southern Platform, **OM**=Ouachita Mountains, **BFZ**=Bahamas Fracture Zone, **LS**=Louann Salt, **CS**=Campeche Salt, **TG**=Triassic Grabens, **MOR**=Mid-Ocean Spreading Ridge.

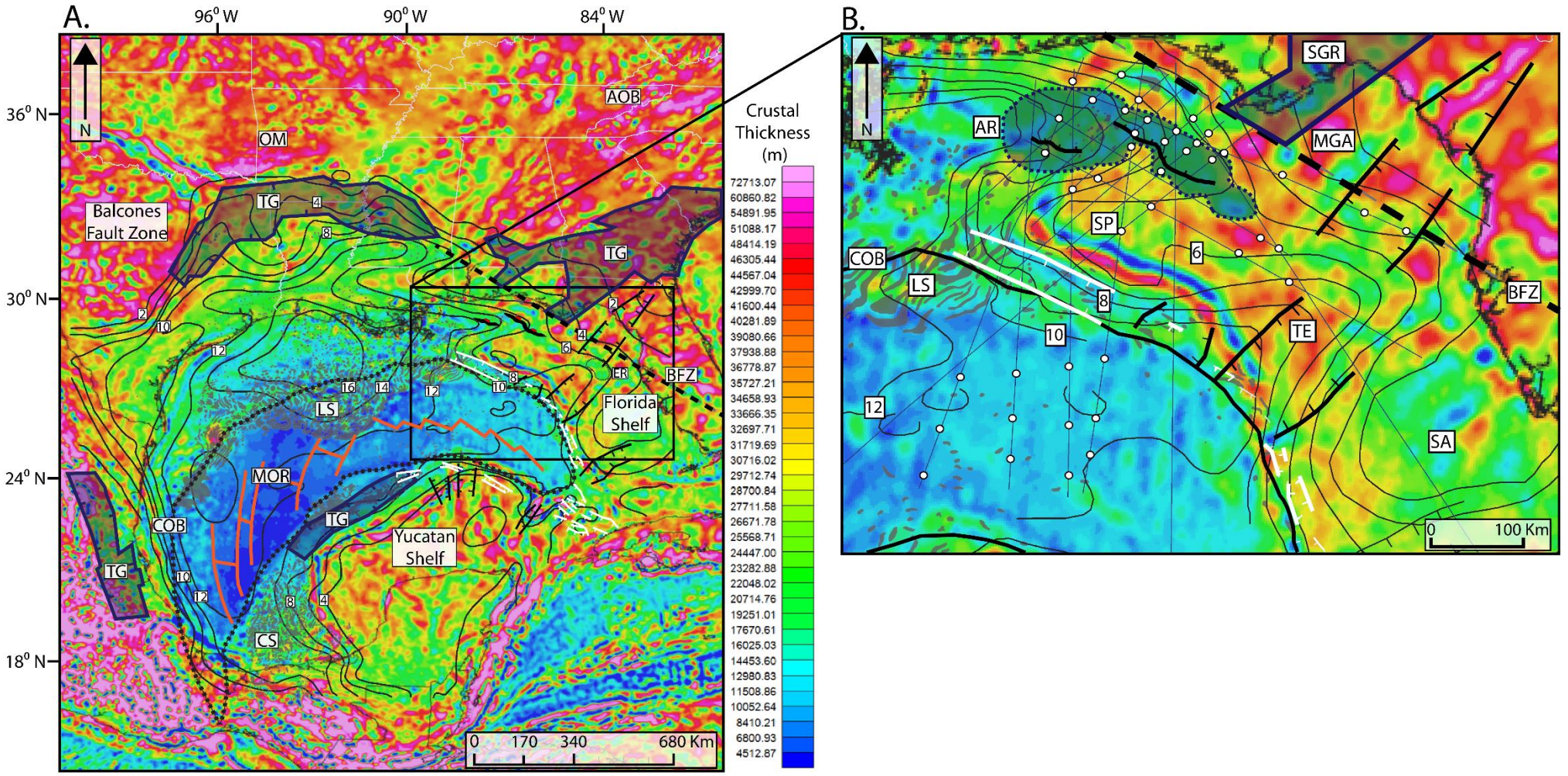
A.
96° W
90° W
84° W
36° N
30° N
24° N
18° N
N
AOB
OM
Balcones
Fault Zone
TG
LS
MOR
COB
CS
Yucatan
Shelf
Florida
Shelf
BFZ
ER
0 170 340 680 Km
Crustal
Thickness
(m)
72713.07
60860.82
54891.95
51088.17
48414.19
46305.44
44567.04
42999.70
41600.44
40281.89
39080.66
37938.88
36778.87
35727.21
34658.93
33666.35
32697.71
31719.69
30716.02
29712.74
28700.84
27711.58
26671.78
25568.71
24447.00
23282.88
22048.02
20714.76
19251.01
17670.61
16025.03
14453.60
12980.83
11508.86
10052.64
8410.21
6800.93
4512.87
B.
N
SGR
AR
MGA
SP
COB
LS
TE
BFZ
SA
0 100 Km

### 2.1.2 Previous work on Mesozoic rifting in the northeast GOM and objectives of this study

The Apalachicola rift (AR) lies largely within the Destin Dome protraction area in the northeast GOM and was proposed by Godo (2017) to form the southwestward extension of the Triassic age South Georgia Rift described by previous workers from the subsurface of Florida and Georgia (Arden, 1974; Applegate and Lloyd, 1985) (Fig. 1A, B). Macrae and Watkins (1995) made seismic interpretations and subsurface maps of the AR that used an older vintage of seismic data that pre-dated my Deep East survey that included their inferences of its syn-rift sedimentary and igneous fill. Both of these previous studies of the AR utilized the same seismic survey that was acquired in 1985 by Digicon Geophysical Corporation and was reprocessed by Fugro in 2014. This 1985 seismic survey has a limited depth penetration especially beneath the locally thick autochthonous Louann salt layer that fills the sag basin above the AR and therefore limits vintage seismic reflection data from the AR.

Hunter (2014) used the Destin Dome Survey and presented a 2D seismic profile of the AR as a half-graben controlled by a low-angle normal fault or "LANF" (Morley, 1989). Eddy et al. (2014) and Liu et al. (2019) interpreted the same regional Deep East line and interpreted the Apalachicola rift as a symmetrical half-graben with inferred igneous flows or "seaward-dipping reflectors". Frederick et al. (2016) summarized the situation in the northern GOM as: "An accurate assessment of the pre-salt structure, sedimentology and stratigraphy in the northeast GOM are crucial for understanding the early opening history of the GOM and how these early rift events impacted subsequent hydrocarbon reservoir seals, traps, and maturation in the northeast GOM".

There are few studies on the Apalachicola rift and geology of the West Florida Shelf since the 1990's as a result of the offshore commercial drilling ban within the Florida moratorium boundary that began in 2006. However, hydrocarbon discoveries on anticlinal highs formed by salt movement in the post-rift section have been made in the late Jurassic Norphlet-Smackover play (Godo, 2017). Gohrbandt (2002) estimates that 32-35 Tcf of dry, undiscovered, recoverable gas resources are estimated to occur elsewhere beneath the northern West Florida Shelf and under the outer Central West Florida Shelf and Slope in the Norphlet-Smackover plays. My study builds on these previous works by making use of the more modern Deep East seismic grid collected by Spectrum (now TGS) in 2007 that provides higher resolution imaging the deeply buried rifts.

## 2.2 Tectonic setting of the northeast Gulf of Mexico

### 2.2.1 Regional tectonic framework from gravity.

As shown in the five-layer, 3D gravity inversion in Figure 1 provided to me by Mei Liu (in prep., 2020), the deep, central GOM oceanic basin is surrounded by an area of highly extended and attenuated crust with the GOM structural limit that is characterized by a sharp transition between thick (32 km) and transitional crust (23 km) in the area of Apalachicola rift in the northeastern GOM (Buffler, 1991; Eddy et al., 2014).

Towards the center of the deep GOM basin, the magnitude of crustal stretching increases and resulted in late Jurassic oceanic crust that formed along an extinct late Jurassic, slow-spreading center with an oceanic crustal thickness range between 4-14 km (Nguyen and Mann,

2016; Lin et al., 2019). The presence of relatively thin continental crust beneath the Apalachicola rift suggests that crustal thinning was more significant in this area than surrounding areas of thicker, transitional, continental crust (Fig. 1).

Variations in depth to the top of the Mohorovicic Discontinuity or "Moho" is one of the main constraints used in the Liu (in preparation, 2020) 3D gravity inversion model and illustrates the shallowing Moho in the northeastern GOM and beneath the central area of oceanic crust (Lin et al., 2019) (Fig 1A, B). On the lines of the Deep East survey, I was able to map the Moho as a package of bright reflectors of varying polarity that range in depth between 30-37 km. In the area of the Apalachicola Rift, the shallower Moho trend forms an area that trends northwest (Fig. 1B).

### 2.2.2 Age control and paleogeography of pre-salt rift deposits

Martin (1978) and Salvador (1987) published the first regional subsurface maps of the GOM, which showed Mesozoic/Triassic rifts around the edges of the basin with their ages based on the palynology of plant remains found in widely-spaced cores (Fig. 1A, Fig. 2). The Triassic-Jurassic paleogeography and the stratigraphic history of the GOM basin are difficult to reconstruct with confidence due to the lack of data from deep wells that penetrate beneath autochthonous salt into "red bed" lithologies of the Eagle Mills Formation in east Texas, Florida and along the eastern margin of North America (Martin, 1978; Salvador, 1987; Godo, 2017; Frederick et al., 2020).

Thick sequences of nonmarine red beds and associated volcanic rocks are known from three main areas within the GOM basin: 1) in the subsurface of South Carolina, Georgia, northwest Florida, and southern Alabama (Arden, 1974; Applegate and Lloyd, 1985); 2) in the

subsurface of southern Arkansas and parts of east Texas, Mississippi, and Louisiana (Frederick et al., 2020); and 3) from outcrops in the exposed and inverted Huizachal-Peregrina and Huayacocotla rifts along the front of the Sierra Madre Oriental of Mexico (Salvador, 1987). Red bed deposits found in the subsurface of the U.S. Gulf coastal plain have been grouped as the Eagle Mills Formation (Frederick et al., 2020); their Mexican stratigraphic equivalents are grouped as the La Boca Formation of the Huizachal Group in east-central Mexico (Fig. 2 from Salvador, 1987). All of these nonmarine red beds are correlated with late Triassic red beds of the Newark Group located along the eastern margin of North America (Dobson and Buffler, 1991).

### 2.2.3 Eastern GOM basement structure

The structural geology of the eastern GOM is characterized by a series of basement highs and lows that represent the combined effect of: 1) late Paleozoic Appalachian collisional event that resulted from the late Paleozoic collision between the North American, South American and African plates that formed the Pangea supercontinent (Pindell, 1985; Frederick et al., 2020); and 2) late Triassic-early Jurassic rifts that formed as the result of Phase 1 rifting episode in the late Triassic that produced northwest-southeast extension both in the GOM and along the eastern margin of North America as shown in Figure 2 (Salvador, 1987; Hunter, 2014; Eddy et al., 2014). These basement highs and lows include from north to south: 1) the Wiggins Arch; 2) the Apalachicola rift; 3) the Middle Ground Arch; 4) the Tampa Embayment and 5) the Sarasota Arch. With the exception of the Wiggins arch all of these basement features lie beneath the extensive area of the West Florida Shelf (Hunter, 2014) (Fig. 2).

A regional 2D seismic line is shown in Figure 3 and crosses the Apalachicola rift, the

Middle Ground Arch, the Tampa Embayment and the Sarasota Arch. Both the Apalachicola rift and the Tampa Embayment exhibit the classical "steer's head geometry" made up of an underlying rift overlain by an unfaulted sag basin that is thickest over the center of the underlying rift (White and McKenzie, 1988; Wilson, 2011; Hunter, 2014). While the Apalachicola rift is imaged on the line, the Tampa rift is inferred as it lies at much greater depth.

Christenson (1990) proposed that the Florida lineament (also called the Bahamas fracture zone by Klitgord et al., 1984) forms the linear, northwest-trending, transition zone between thicker continental crust (32 km) in Florida and the thinner, transitional crust (26 km) beneath the West Florida platform (Fig. 1A, Fig. 2). Christenson (1990) observed that this lineament forms sharp truncations of regional magnetic and gravity anomalies as shown in Figure 1A and exhibits abrupt changes in basement types and ages across the zone (Fig. 2). Christenson (1990) notes that the lack of major, strike-slip offsets of pre-Mesozoic basement terrains across the Florida Lineament indicates that the lineament likely represents a Triassic-Jurassic age, extensional rift margin.

**Figure 2.** Basement rock types of eastern GOM including sedimentary late Triassic-early Jurassic, Phase 1 rifts from Salvador (1987). This map displays the eastern GOM structural highs and lows of the top basement surface that can be attributed to remnant deformational effects of late Paleozoic collision that formed Pangea and/or Triassic-Early Jurassic Phase 1 extension. Depth to basement contours modified from Sawyer et al. (1991). Lithologies and wells are compiled from Lin (2018), Applegate and Lloyd (1985), Pindell (1985) and Christenson (1990).

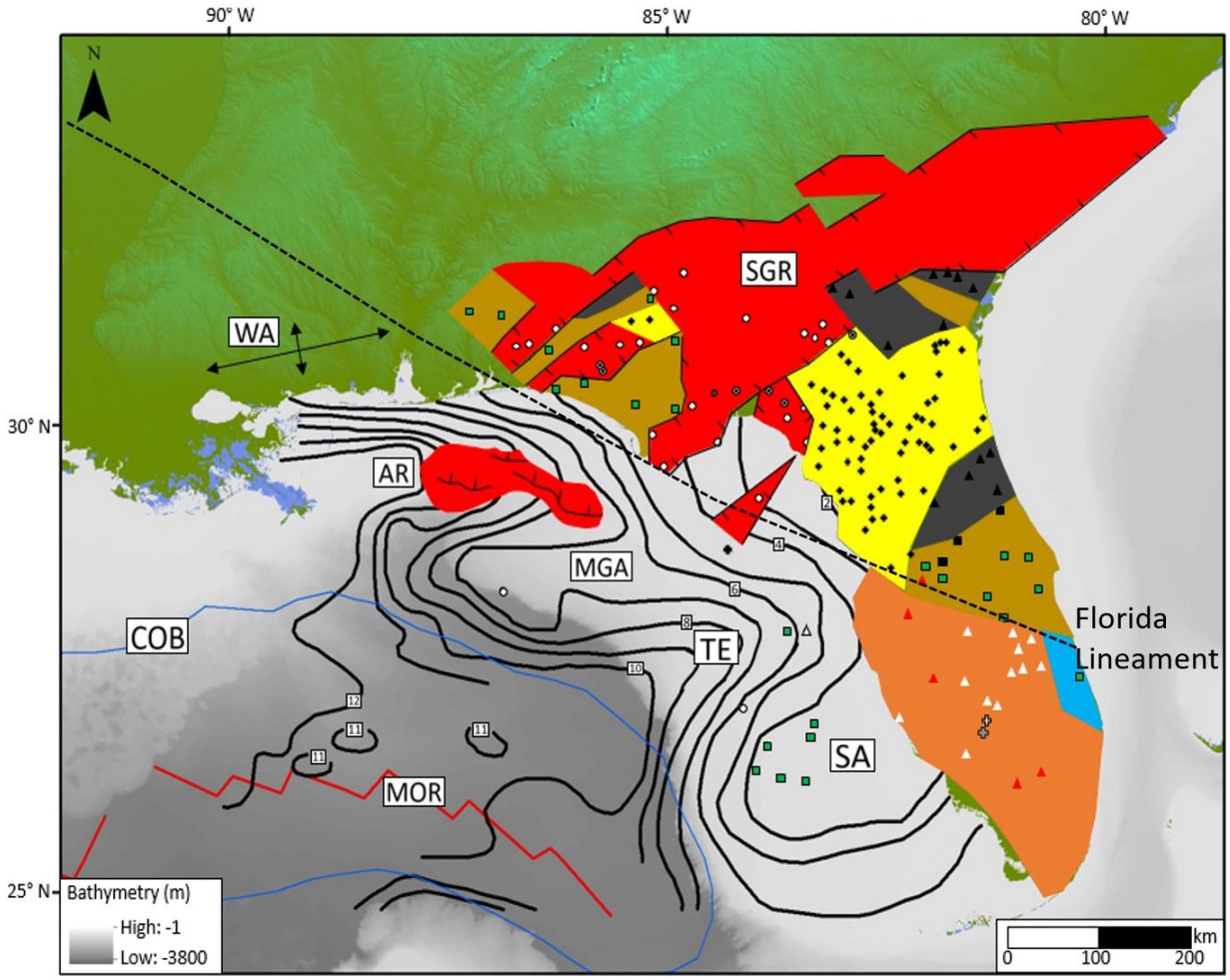


- Triassic-Jurassic clastic and volcanic rocks
- Lower Paleozoic sedimentary rocks
- Lower Paleozoic tuffaceous sedimentary rocks
- Paleozoic(?) rhyolites and felsic volcanics
- Paleozoic(?) diorites and mafic plutonics

Precambrian-Ordovician

- Ordovician-Dev. sedimentary rocks
- Osceola volcanic complex
- Osceola granite
- St. Lucie complex

- Paleozoic/Mesozoic granites
- Jurassic volcanic rocks
- Late Jurassic Wood River Formation
- Jurassic volcanics rocks overlain by Wood River Formation

Mesozoic

- Continental sedimentary rocks
- South Florida volcanic province

### 2.2.4 Pre-middle Jurassic and basement rocks of EGOM and Florida

The base of the late Jurassic Louann Salt represents a relatively smooth unconformity and has been used to define the "top basement" in the previous study by Dobson and Buffler (1991) of the eastern GOM. This top basement surface was likely the consequence of the limited resolution of seismic imaging during the 1980s and 1990s rather than representing a true “top basement” (Lin, 2018). In this study, I refer to this boundary as the mid-Jurassic unconformity formed during the beveling of topography following late Triassic-early Jurassic rifting.

Only in the northeastern, eastern and southeastern parts of the offshore GOM is crystalline, Paleozoic basement shallow enough to be encountered by wells as shown in Figure 2 (Arden, 1974; Applegate and Lloyd, 1985; Christenson, 1990; Dobson and Buffler, 1991; Lin, 2018). The basement terrain of the southern Peninsular Florida is characterized by Lower Cambrian to Precambrian granite and Lower Jurassic volcanic rocks (Christenson, 1990). In offshore areas along the West Florida Shelf, several wells have penetrated below the mid-Jurassic unconformity and documented the underlying late Paleozoic igneous rocks (Godo, 2017). The Paleozoic rocks in Florida are an inherited remnant of the African plate and for this reason have similar lithologic age in the Ordovician Bove basin of Guinea in west Africa (Boote and Knapp, 2016; Godo, 2017).

Figure 4 shows a regional seismic line that crosses the Apalachicola rift and the Middle Ground Arch as a strike view and includes the location of the FM-252 well that penetrates over 450 m of Ordovician clastic rocks that were cored at the bottom of the Texaco-1 well located on the Middle Ground Arch (Christenson, 1990; Godo, 2017). Based on this Texaco well, an inferred boundary between the pre-rift Paleozoic clastics and basement can be interpreted across

the line as the FM-252 bottomed in Paleozoic clastic rocks without encountering an igneous basement.

**Figure 3**. **A.** Uninterpreted northwest-trending seismic line DE-373 across the West Florida Shelf and southern part of the Apalachicola basin (location of line shown on map in Figure 5) **B.** Interpreted seismic line from A showing the basement structure beneath the West Florida Shelf. The areas of the Apalachicola rift and Tampa Embayment (that is inferred to be underlain by a deeply-buried rift) are separated by the basement high of the Middle Ground Arch that is characterized by thicker crust and a thinner, overlying, passive margin section. The Apalachicola rift contains a thinner ~600-1000 meter-thick sequence of Louann Salt. This same salt unit thins and disappears entirely across the Middle Ground arch and southward across the West Florida Shelf.

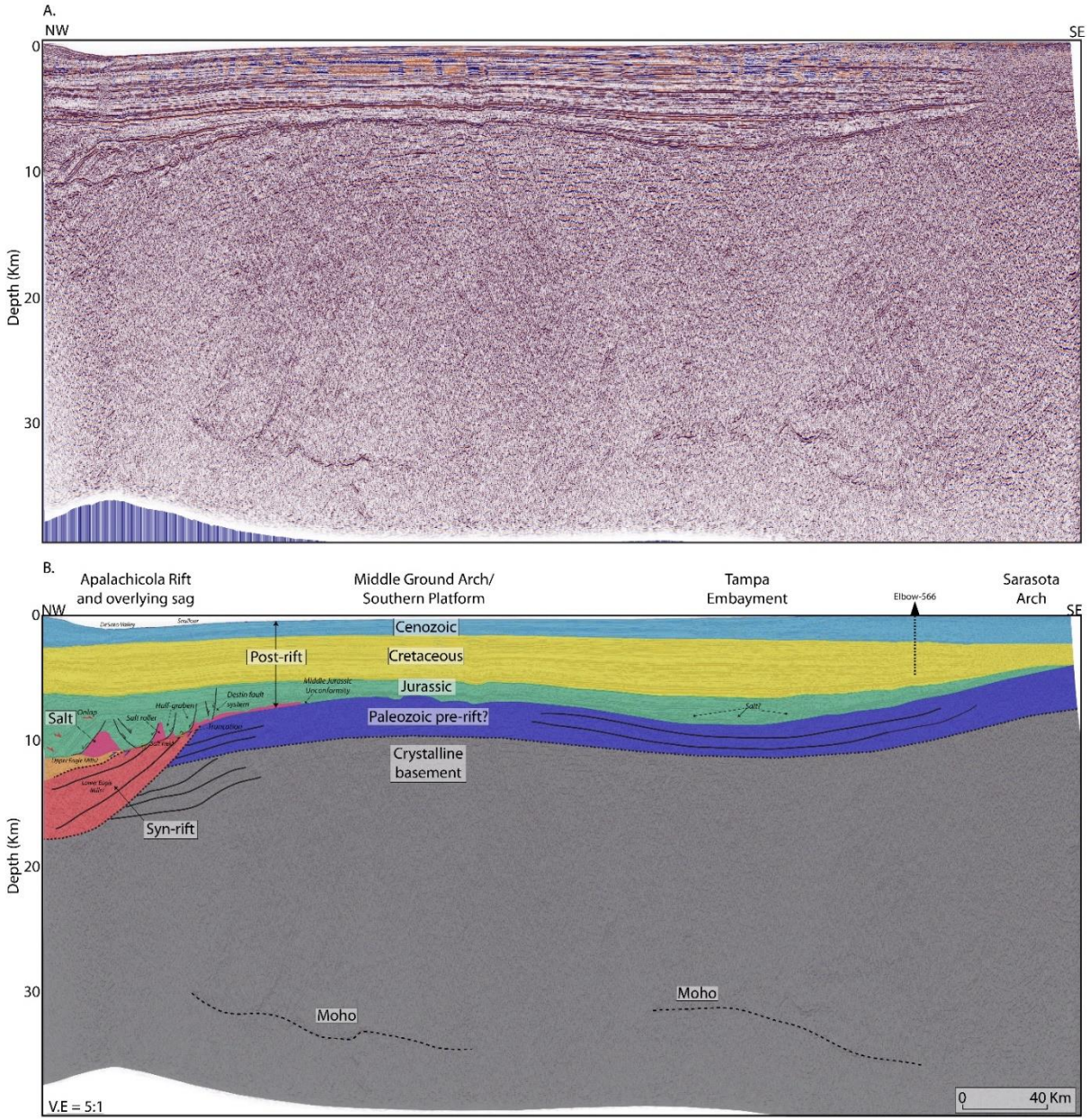
A.
NW
SE
0
10
20
30
Depth (Km)
B.
Apalachicola Rift
and overlying sag
Middle Ground Arch/
Southern Platform
Tampa
Embayment
Elbow-566
Sarasota
Arch
NW
SE
Cenozoic
Post-rift
Cretaceous
Jurassic
Middle Jurassic
Unconformity
Destin fault
system
Half-grabens
Salt
Onlap
Salt roller
Translation
Paleozoic pre-rift?
Salt?
Crystalline
basement
Syn-rift
Moho
Moho
V.E = 5:1
0
40 Km

### 2.2.5 Late Triassic Eagle Mills Formation

The Eagle Mills formation represents a late Triassic, siliciclastic, fluvial red bed formation that was deposited during Phase 1 rifting of the GOM opening (Martin, 1978; Salvador, 1987; Godo, 2017; Frederick et al., 2020). The Eagle Mills formation has been identified onshore in gravity and magnetic-defined rift troughs extending from northeast Texas across southern Arkansas and Mississippi (Godo, 2017; Frederick et al., 2020).

Phase 1 rift basins that occur along the eastern margin of North America also contain fluvial and lacustrine red beds referred to as the Newark Supergroup with deposits consisting of conglomerate, sandstone, and siltstone with occasional lacustrine mudrock as well as basalt intrusions related to the early Triassic (~201 Ma) Central Atlantic Magmatic Province, or "CAMP" (Marzoli et al., 2009). Initial detrital zircon analysis to determine sediment provenance for the Eagle Mills formation around the northern GOM and similarly for the Newark Supergroup along the eastern margin of North America indicate a source terrains that include the northern and western Ouachita highlands, the southern Sabine and Monroe arches, and Gondwanan and Gondwana-affinity source areas based on the African-Amazonian lithospheric composition of the Suwannee terrane (Frederick et al, 2020). Frederick et al. (2020) interpret that thickness and distribution of the Eagle Mills Formations was controlled by remnant late Paleozoic orogenic topography or "successor basins" rather than Triassic-early Jurassic, low-angle normal faults (LANFs) as described from along the eastern margin of North America.

### 2.2.6 Wells drilled into Triassic-Jurassic rifts

The Gainesville 707 well drilled by Sohio in 1985 and the Sake #2 well drilled near DeSoto Canyon are the only deep wells that document Triassic-age syn-rift deposits in the offshore regions of the GOM. The GV-707 Sohio well drilled 4775 ft beneath the Jurassic unconformity into a half-graben and recorded continental red beds, siltstone and volcaniclastic rocks with basalt intrusions - but revealed no evidence for lacustrine or marine shale with source rock potential (Applegate and Lloyd, 1985; Godo, 2017). The palynology report for this well assigned a late Triassic (Carnian) age after analysis of spores and bisaccate pollen similar to Triassic continental red bed sequences in Virginia, Colorado, Utah, and Texas. The Sake #2 well encountered a 262 ft interpreted section of the Eagle Mills Formation with occasional red beds interbedded with light to dark gray fine-grained sandstone that is underlain by a slightly calcareous silty shale section with abundant traces of volcanic ash as well as blocky anhydrite (Frederick et al., 2016). This section of Eagle Mills could represent the filling of sag basins that marked the transition between the fault-controlled rift and the overlying, unfaulted sag basin (Godo, 2017).

**Figure 4**. **A.** Uninterpreted northwest-trending seismic line DE-380b across the northern section of the Apalachicola basin and West Florida Shelf (location of line shown on map in Figure 5). **B.** Interpreted seismic line from A illustrating strike view of Apalachicola rifts that shows characteristic intra-basin highs and lows. Well FM-252 was drilled by Texaco and cored Lower Ordovician clastic rocks consisting of sandstone units overlain by black or dark gray shale that underlie the prominent, mid-Jurassic unconformity (Arden, 1974). An approximate boundary between pre-rift sediments and basement is shown based on Arden (1974).

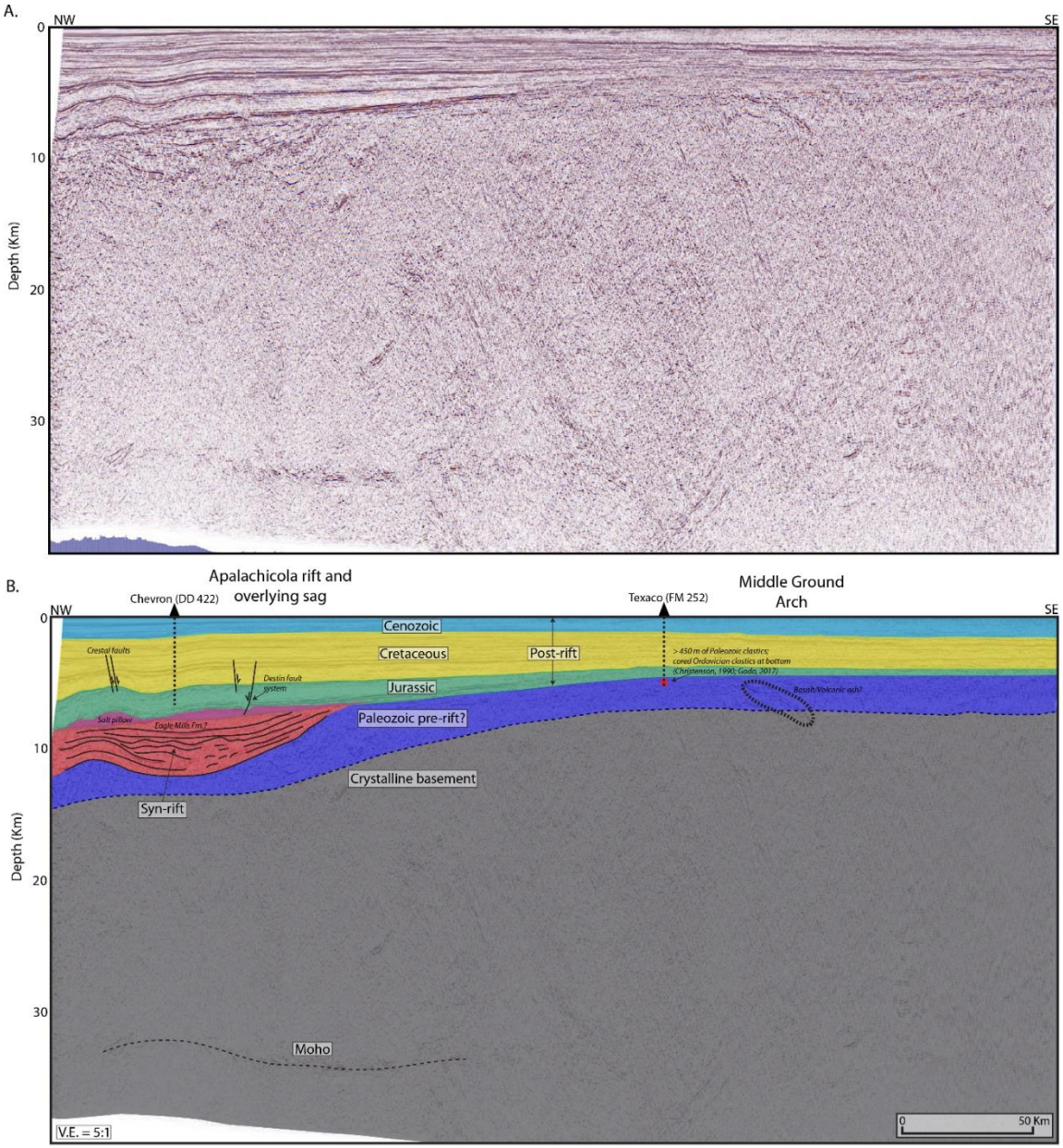
A.
NW
SE
0
10
20
30
Depth (Km)
B.
Apalachicola rift and
overlying sag
Chevron (DD 422)
Texaco (FM 252)
Middle Ground
Arch
NW
SE
Cenozoic
Cretaceous
Jurassic
Post-rift
Paleozoic pre-rift?
Crystalline basement
Syn-rift
Moho
Crestal faults
Destin fault
system
Salt pillow
Eagle Mills Fm?
> 450 m of Paleozoic clastics;
cored Ordovician clastics at bottom
(Christenson, 1990; Goda, 2017)
Basalt/Volcanic ash?
V.E. = 5:1
0
50 Km

## 2.3 Dataset and methods used in this study

### 2.3.1 Seismic reflection grid.

This study uses approximately 7,600 line-km of the 36,000 line-km 2D seismic reflection "Deep East survey" that was collected in 2007. The data has been pre-stack depth migrated by Spectrum (now TGS) to investigate the Apalachicola rift architecture and stratigraphy as summarized in Figure 5.

The same seismic survey covers much of the West Florida Shelf, the shelf break and slope, and extends southward into the central, oceanic GOM (Lin et al., 2019; Liu et al., 2019). The seismic data have a maximum depth penetration around 30-40 km that allows for sufficient imaging and interpretation of pre-salt rift features that include the top basement (Jurassic unconformity) and in some areas - the Moho (Fig. 1B, Fig. 3B). These 2D seismic transects are generally oriented perpendicular to the shelf break.

### 2.3.2 Wells used in the study.

Within the Apalachicola Basin area, there are no wells that penetrate beneath the Middle Jurassic unconformity - thus the inferred syn-rift lithology comes from the nearby Sohio GV-707 well, Sake #2, onshore penetrations in the SGR and in the Texas-Louisiana-Arkansas region (Arden, 1974; Applegate and Lloyd, 1985; Pindell, 1985; Christenson, 1990). Five industry wells in the overlying sag basin with a maximum penetration to the top salt horizon are used to correlate the various ages ranging from the middle Jurassic to present-day sedimentary rocks.

I have also used as guides the previously published seismic lines of Dobson and Buffler

(1997), Hudec et al. (2013), Hunter et al. (2014), Snedden and Galloway (2019) and personal communications from Ted Godo (2020).

One industry well is located in the Tampa Embayment area and was used for post-salt correlations on the regional seismic line across the eastern GOM (Fig. 3). The FM-252 well is also used to document a Paleozoic penetration beneath the mid-Jurassic unconformity (Fig. 4). The identification of rift features such as normal faults and overlying sag relied on mapping of the 2D seismic grid which has an average line spacing of 20 km.

### 2.3.3 Potential fields data

Gravity and magnetic data from Sandwell et al. (2009) and Fugro Inc. (2007) were used to delineate basins, arches, edges, faults, crustal thickness and denser materials such as crystalline rocks or igneous intrusions in the eastern GOM region.

**Figure 5.** The locations of seismic lines and well data are shown on a bathymetric basemap of the northeastern GOM. The Deep East seismic reflection survey was provided by Spectrum (now TGS) and consists of a ~35,000 line km 2D PSDM reflection survey with depth penetrations down to the Moho (~30-40 km). I have used 15 lines from that survey to investigate rifting beneath the Apalachicola basin. The seismic lines labeled with figure numbers are shown later in this chapter. Six wells in the overlying Apalachicola post-rift sag were used to correlate stratigraphy beneath the top Louann salt. Nearby wells in the Tampa Embayment and from previous studies (Hunter, 2014; Godo, 2017; Lin, 2018) were used to correlate Mesozoic and Cenozoic units across the West Florida Shelf. The Sohio (GV-707) and Sake #2 (DC) are used as offshore Triassic sediment analogs for the Apalachicola pre-salt sediments. Wells further to the southeast include top Paleozoic basement penetrations and are described by Christenson (1990). Black faults represent the main half-graben normal faults from this study: AR in northwest and Elbow rift in southeast. Gray faults represent extensional post-rift salt tectonics from Pashin et al. (2016). **SGR**=South Georgia Rift, **BFZ**=Bahamas Fracture Zone, **COB**=Continent-Ocean Boundary, and **MOR**=Mid-Ocean Ridge.

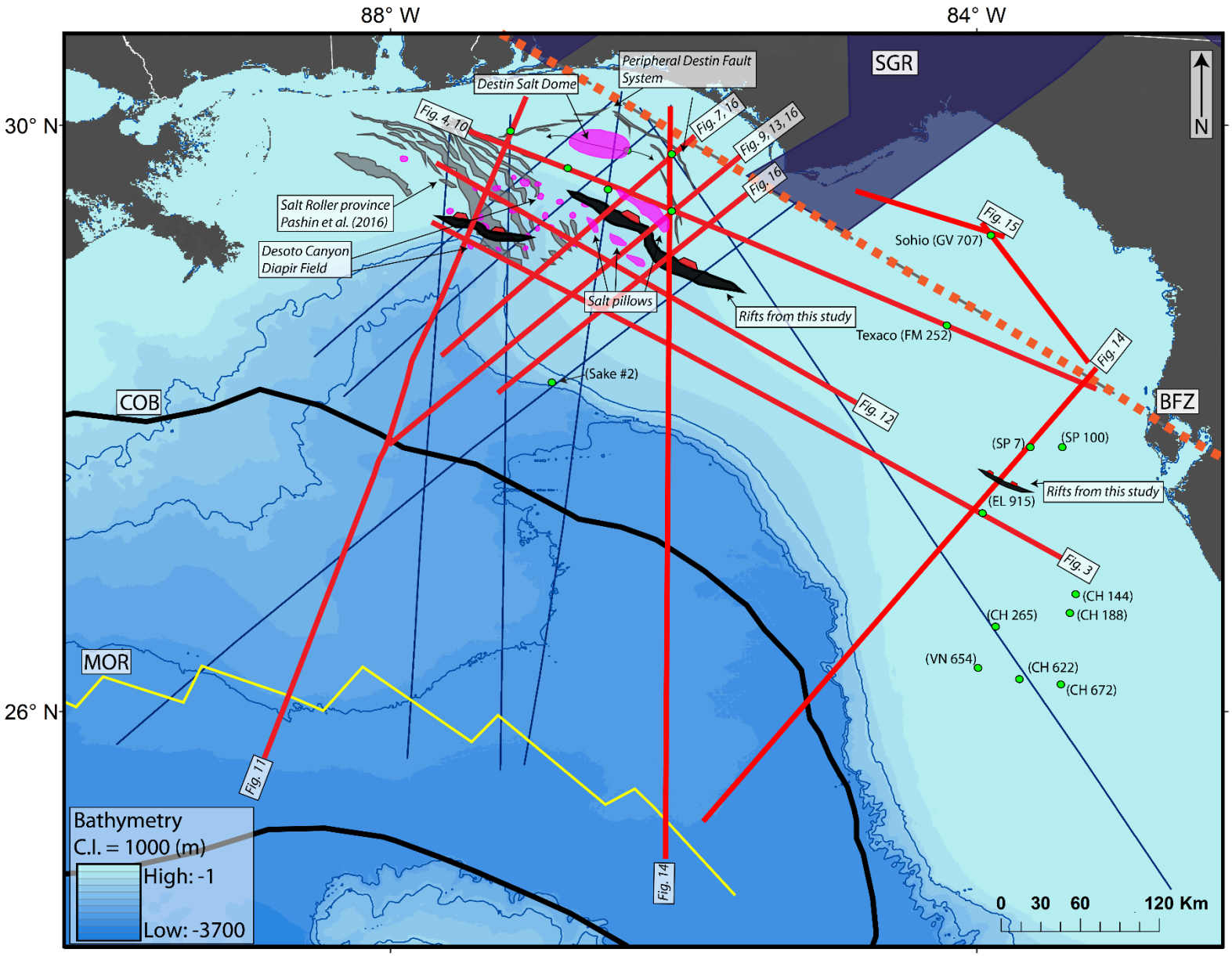
88° W
84° W
30° N
26° N
N
SGR
Peripheral Destin Fault System
Destin Salt Dome
Fig. 4, 10
Fig. 7, 16
Fig. 9, 13, 16
Fig. 16
Salt Roller province
Pashin et al. (2016)
Desoto Canyon
Diapir Field
Salt pillows
Rifts from this study
Sohio (GV 707)
Fig. 15
Texaco (FM 252)
Fig. 14
(Sake #2)
COB
Fig. 12
BFZ
(SP 7)
(SP 100)
Rifts from this study
(EL 915)
Fig. 3
(CH 144)
(CH 265)
(CH 188)
MOR
(VN 654)
(CH 622)
(CH 672)
Fig. 11
Fig. 14
Bathymetry
C.I. = 1000 (m)
High: -1
Low: -3700
0 30 60 120 Km

## 2.4 Post-Phase 1 sag basin overlying the Apalachicola rift

### 2.4.1 Sag phase and salt infill

After Phase 1 rifting ended in the early Jurassic, the GOM entered its "sag phase" in which marine waters entered the large bowl-shaped topographic either from the Pacific ocean and through the Balsas portal in central Mexico (Salvador, 1987; Dobson and Buffler, 1997; Godo, 2017; Steier and Mann, 2019) – or, alternatively, from the proto-Atlantic Ocean through a corridor in the southeastern GOM (Snedden and Galloway, 2019).

The combination of an arid climate and shallow saltwater seas/lakes allowed for saltwater evaporation and subsequent precipitation of an extensive salt body over much of the GOM during the late Bathonian-Callovian (Salvador, 1987; Dobson and Buffler, 1997). The Louann-Campeche salt deposition is thickest in the western and central GOM and thins towards the northeast GOM where the DeSoto and Destin Dome salt basins occur. Salt thins and disappears completely at the easternmost extent of the onshore Apalachicola Embayment (Godo, 2017; Steier and Mann, 2019).

### 2.4.2 Remobilized salt in the sag basin overlying the Apalachicola rift

Remobilized salt related to gravity spreading during the Jurassic to present day is responsible for many structures in the northeast GOM that include salt rollers, salt pillows, salt diapirs, and extensional fault systems. Remobilized salt and its associated structures is the mechanism for the formation of structural traps of the major oil discoveries of the Norphlet-Smackover play within the Destin Dome (MacRae and Watkins, 1992; Dobson and Buffler, 1997; Godo, 2017).

### 2.4.3 Passive margin section overlying the Apalachicola rift and sag basin

The overlying post-rift, passive margin strata in the Apalachicola basin consists of a 3-5 km thick Jurassic section containing the Louann Salt, Norphlet sandstone, Smackover carbonate, and Haynesville shale formations that were deposited during Phase 2 rifting of the GOM as summarized on the stratigraphic column for the GOM shown on Figure 6.

The Cotton-Valley Knowles formation is a mixed section of sandstone and limestone and was deposited in the period around the Jurassic-Cretaceous boundary. The Cotton-Valley Knowles formation was subsequently buried by the deposition of an approximate 5-6 km thick, Cretaceous, passive margin section that accompanied Phase 2 oceanic spreading. The Jurassic-earliest Cretaceous depositional sequence ended with a significant drop of relative sea level and is marked by a major unconformity (Dobson and Buffler, 1997).

The Sligo-Hosston formations marks the initiation of the passive margin phase in the eastern GOM. The Cretaceous/Paleogene (K/P) boundary is marked by the top of the shale-dominant Selma formation (Mancini et al., 2001). Since the early Miocene, the western section of the Apalachicola basin has received rapid, clastic sedimentation from the eastern lobe of the Mississippi Delta (Hunter, 2014).

**Figure 6.** Generalized stratigraphy for the eastern GOM modified from Lin (2018). Because there are no well penetrations beneath the post-rift Louann Salt in the Apalachicola area, the Apalachicola syn-rift section (Eagle Mills Formation) is inferred from seismic reflection data. Phase 2 rifting post-dated Louann Salt deposition and included late Jurassic units such as the Norphlet, Smackover, Haynesville, and Cotton-Valley formations. Following the Jurassic rift and sag, a thick (~5 km) carbonate-clastic sequence of the Cretaceous passive margin was deposited.

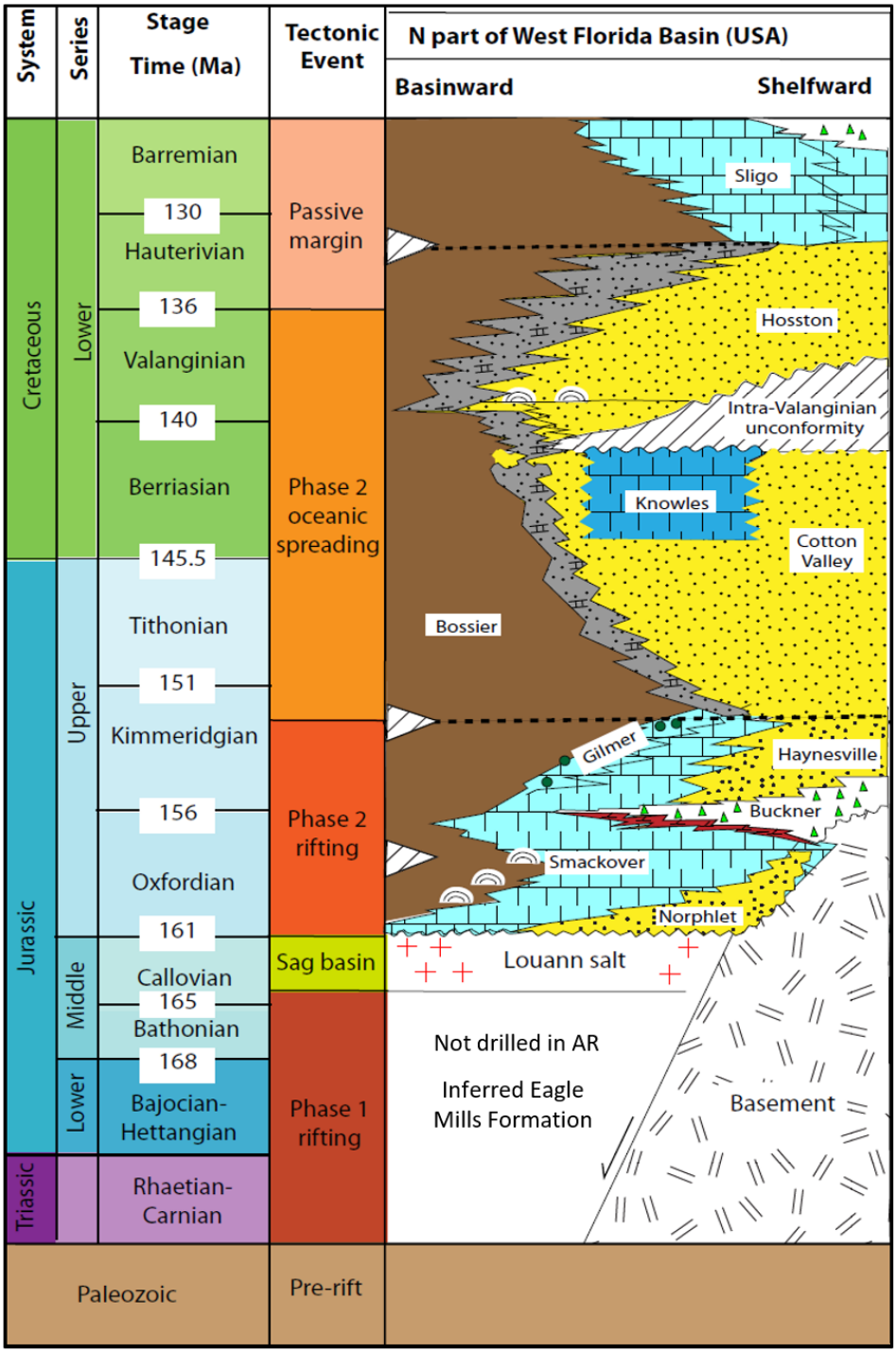
System
Series
Stage
Time (Ma)
Tectonic Event
N part of West Florida Basin (USA)
Basinward
Shelfward
Cretaceous
Lower
Barremian
130
Hauterivian
136
Valanginian
140
Berriasian
145.5
Passive margin
Phase 2 oceanic spreading
Jurassic
Upper
Tithonian
151
Kimmeridgian
156
Oxfordian
161
Phase 2 rifting
Middle
Callovian
165
Bathonian
168
Sag basin
Lower
Bajocian-Hettangian
Phase 1 rifting
Triassic
Rhaetian-Carnian
Paleozoic
Pre-rift
Sligo
Hosston
Intra-Valanginian unconformity
Knowles
Cotton Valley
Bossier
Gilmer
Haynesville
Buckner
Smackover
Norphlet
Louann salt
Not drilled in AR
Inferred Eagle Mills Formation
Basement
Sandstone
Shale
Anhydrite
Louann Salt
Basement
Carbonate Reefs
Red Dolomitic Claystone
Absent
Grey Calc Siltstone
Shallow Water Limestone
Oolitic Limestone

### 2.4.4 Late Jurassic sag basin overlying the Apalachicola rift as imaged on seismic data

The sag deposits overlying the Apalachicola rift are well shown on a northeast-trending seismic profile shown in Figure 7. The stratigraphic correlations are based on the Destin Dome Block 166 well which penetrated down to the top of Louann Salt (T. Godo, personal communication, 2020).

Anticlinal and dome-like features were created as gravity sliding and sediment loading caused the Louann salt body to remobilize and migrate into in the center of the sag depression as dome-shaped, salt pillows, salt rollers, and salt diapirs (Pashin et al., 2016). These gravity-driven, downward movements of the thicker salt bodies into the center of the sag basin created salt withdrawal features around the more elevated margins of the sag basin and led to a downwarped "Top Tithonian" horizon (Fig. 7).

On the northeastern side of the seismic line shown in Figure 7, the initiation of the Destin Dome salt anticline formed by up-dip, counterflow of middle Jurassic salt towards the eastern basin margin in response to Lower Cretaceous differential sediment loading and basin subsidence through time (MacRae and Watkins, 1992). The extent of Destin Dome salt anticline east of the AR is shown on the regional map in Figure 5.

The most northeasterly normal fault with a basinward dip towards the southwest represents the up-dip limit of salt tectonics and can be traced around the periphery of the GOM basin in the southeastern USA as a continuous normal fault as discussed by Dobson and Buffler (1997) (Fig. 5). This peripheral normal fault system marking the up-dip limit of salt is also known as the Destin Fault System (Pashin et al., 2016). Below the mid-Jurassic unconformity

lies the half-graben of the AR with its southwest-dipping internal, syn-rift reflections and is discussed in greater detail in the next section on its half-graben architecture and fault geometry (Fig. 9).

Although no well has penetrated the mid-Jurassic unconformity into the syn-rift section of the AR, I infer a depositional environment within an arid setting with non-marine red bed deposition of the late Triassic-age Eagle Mills Formation (Frederick et al., 2020). Similarly, the underlying pre-rift section is inferred to be Paleozoic metasedimentary and igneous rocks - although no distinctive seismic reflector is visible separating Paleozoic sedimentary rocks from crystalline basement. There is no seismic evidence for additional normal faults southwest of the AR since this is the area of the unfaulted Southern Platform (Godo, 2017) (Fig. 5).

**Figure 7**. **A.** Uninterpreted northeast-trending seismic line DE-1699 across the Apalachicola basin and rift (location of line shown on map in Figure 5) **B.** Interpreted northeast-trending seismic line from A that illustrates the post-rift stratigraphy in the Apalachicola basin. The sag basin is characterized by a relatively thin (~3 km) sequence of Jurassic sedimentary rocks overlain by a thicker (~5 km) Cretaceous sequence. Salt tectonics controls many potential hydrocarbon traps as shown by salt withdrawal from up-dip, domal structures which creates a zone of thickening in the downdip, Cretaceous center of the sag. Salt rollers, salt pillows, and diapirs are also prevalent throughout the basin. The southwest-dipping normal fault on the northeastern end of the seismic line is called the Destin fault system (Pashin et al., 2016) and represents the up-dip limit of salt tectonics due to gravity sliding and sediment loading that rims around the periphery of the Apalachicola basin. Moving southwestwards away from the half-graben, there is little evidence for faults or tilted fault blocks as the crust there largely represents the thicker crustal area of the Southern Platform.

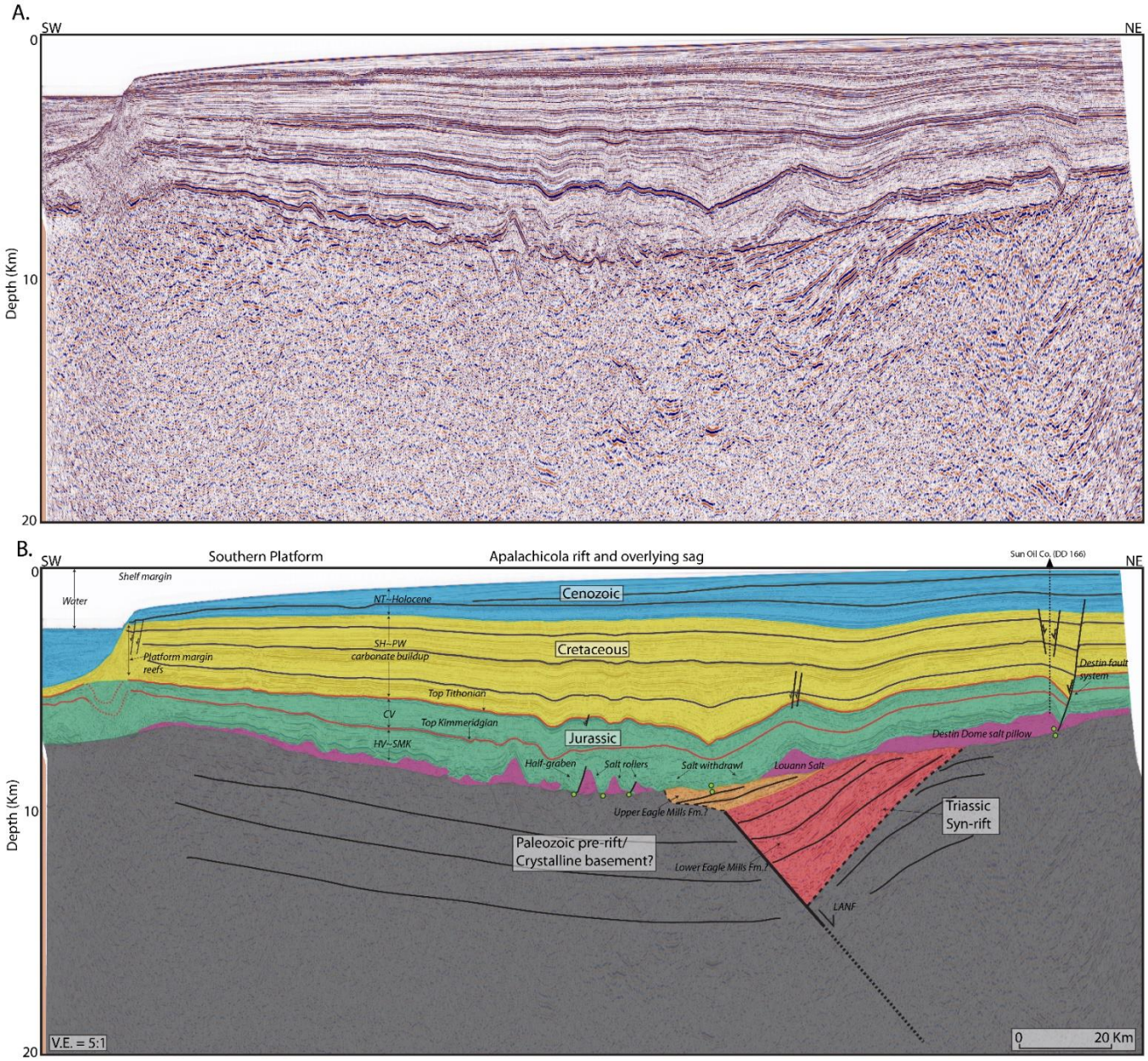
A.
SW
NE
0
10
20
Depth (Km)
B.
SW
Southern Platform
Apalachicola rift and overlying sag
Sun Oil Co. (DD 166)
NE
0
Shelf margin
Water
NT–Holocene
Cenozoic
SH–PW
carbonate buildup
Cretaceous
Platform margin
reefs
Destin fault
system
Top Tithonian
CV
Top Kimmeridgian
Jurassic
HV–SMK
Destin Dome salt pillow
Half-graben
Salt rollers
Salt withdrawl
Louann Salt
Upper Eagle Mills Fm.?
Triassic
Syn-rift
Paleozoic pre-rift/
Crystalline basement?
Lower Eagle Mills Fm.?
LANF
10
20
Depth (Km)
V.E. = 5:1
0
20 Km

### 2.4.5 Regional subsurface structural maps of the Apalachicola rift

Structure maps of key surfaces shown in Figure 8 show that the Apalachicola rift faults exhibit an east-southeast to west-northwest trend. The deepest syn-rift sections of the AR are found on the western end of the survey area and towards the central GOM. The syn-rift sections shallow eastwards in the direction of the modern Florida shoreline where the edge of the sag basin is defined by the up-dip limit of salt in the onshore Apalachicola Embayment (Fig. 8F). Similar maps of the AR orientation and its eastward shallowing of the syn-rift section have been mapped by Dobson and Buffler (1997) and Hunter (2014).

A structure map for the base of the syn-rift was created by mapping the approximate boundary between the syn-rift and pre-rift as shown on the map in Figure 8E. Some seismic profiles contain bright reflectors that likely indicate the syn-rift and pre-rift boundary, although in some cases this boundary mapping involves analyzing the up-dip extent of dipping reflectors and looking for wedging versus parallel, non-growth strata. The syn-rift orientation and trend follow the northwest-trending shallow Moho surface that was mapped using the deeper Moho reflectors from the seismic grid.

The bounding LANF's of the AR exhibit a northwest-trend with the westernmost, listric normal fault accounting for a larger amount of accommodation space within the syn-rift section (Fig. 8F). The highs along the southern area of the structure maps represent the unfaulted and higher standing Southern Platform as also shown on the maps in Figures 2 and 3.

An isopach for the base of the syn-rift and the overlying mid-Jurassic unconformity is shown in Figure 8F. In this figure, syn-rift sedimentation is thickest in the western part of the rift

with an average thickness between 6,900 and 7,800 m and a maximum thickness between 7,800 and 8,600 m. The easternmost section of the syn-rift has an average thickness between 6,000 and 6,900 m (Fig. 8F).

**Figure 8.** Structure maps for the Callovian, Oxfordian, Kimmeridgian, and Tithonian periods in the area of the early Phase 1 Apalachicola rift illustrating sediment fill in the basin. **A. Mid-Jurassic unconformity.** This map represents the period time immediately after Phase 1 rifting and is evident as a relatively smooth erosional unconformity that is mappable along the west Florida Shelf. **B. Top Oxfordian**. Marks the top of the Smackover carbonates and Norphlet sandstone formations that lie above the Louann Salt and together represent the early stages of basin fill in this area. **C. Top Kimmeridgian**. Deposition of the Haynesville formation which primarily includes sandstone fill on the shelf and shale towards the GOM basin. **D. Top Tithonian.** Represents the base of the Cretaceous section and includes the deposition of Cotton-Valley formation which consists primarily of sandstone in the basin. The overlying post-rift has an east-west trend and contains deeper sections seaward. **E.** The **base syn-rift map** shows a northwest orientation of this surface which parallels the shallowing Moho/gravity trend under the rift as shown in Figure 1. **F.** An isopach between the base syn-rift and mid-Jurassic unconformity surfaces reveals up to around 6-7 km of syn-rift thickness in these rifts. Seismic interpretations show syn-rift thicknesses up to 10 km depending on the exact depth of the syn-rift/pre-rift boundary.

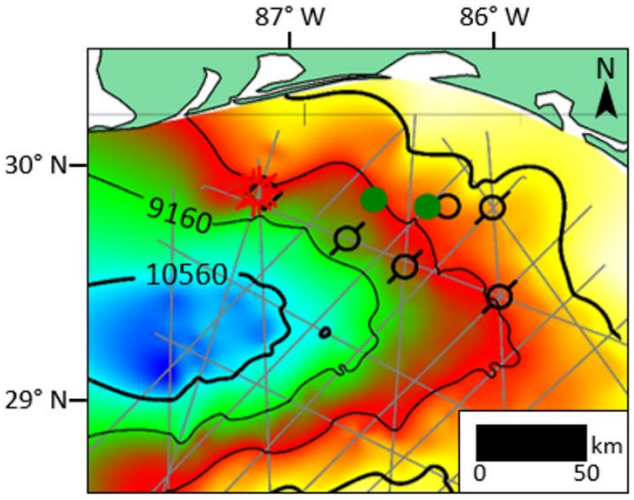


A. Upper Jurassic unconformity

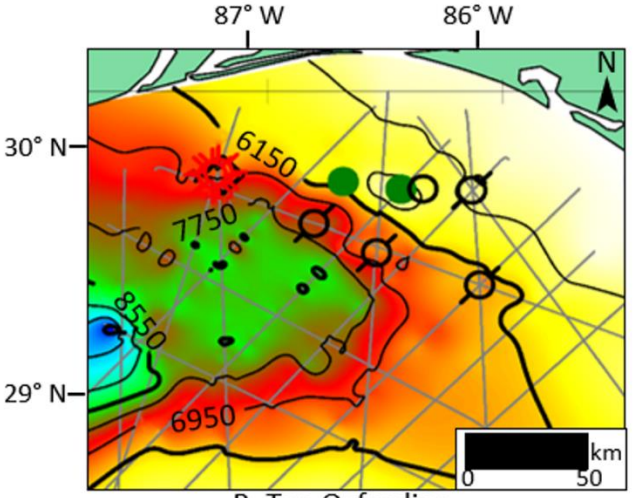


B. Top Oxfordian

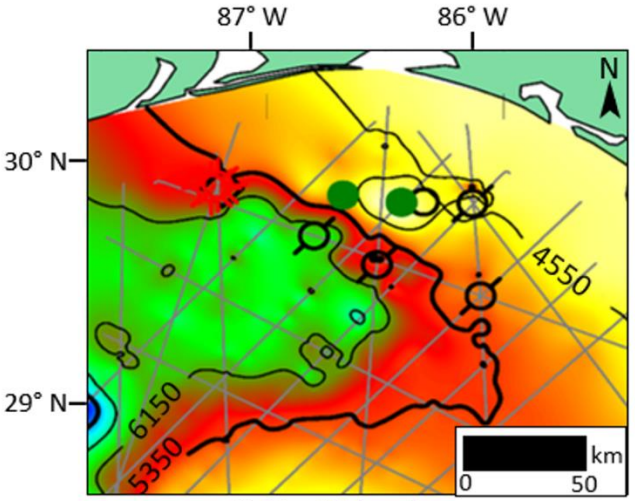


C. Top Tithonian

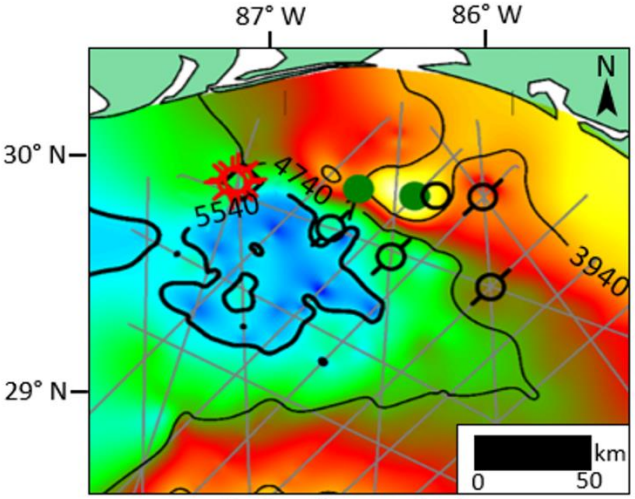


D. Top Kimmeridgian

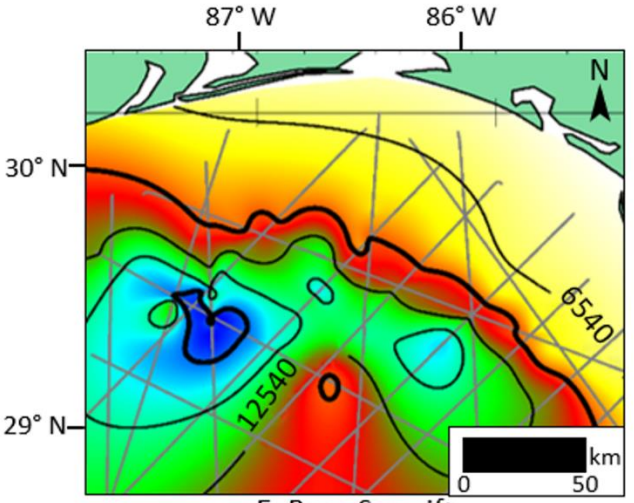


E. Base Syn-rift

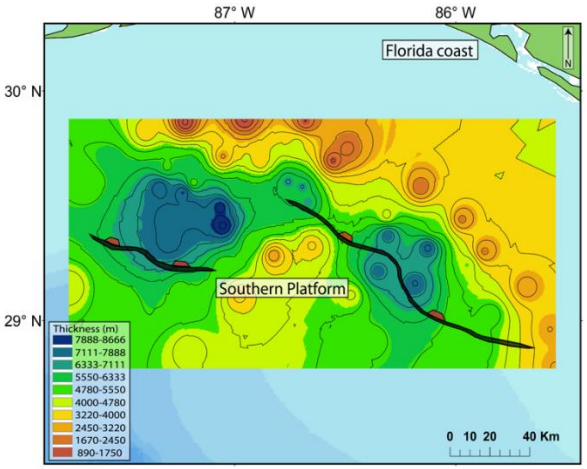


F. Syn-rift isopach

## 2.5 Structure of the pre-salt Apalachicola rift in the northeastern Gulf of Mexico

### 2.5.1 Fault geometry of half-grabens

The Apalachicola rift is largely controlled by two major, *en echelon* half-graben normal faults that have a general northwest-southeast trend and dip toward the northeast (Figs. 7, 8). Dip angles for both of these LANFs range from 31°-33° (Fig. 9) - as also observed by Withjack et al. (2013) from coeval Triassic rifts along the eastern margin of North America. Morley (1989, 2009) also observes similar dip angles in examples of presently-active LANF's from East Africa and Thailand.

Figure 9 illustrates a northeast-trending dip line that contains a large, listric normal fault dipping 33° to the northeast and detaching at depth of about 20 km. This normal fault is part of a 136-km-long normal fault system in the eastern part of the basin that trends in a northwest-direction. The maximum thickness of the syn-rift on this line is approximately 6 km.

The syn-rift infill of this rift is characterized by noticeable stratigraphic wedging adjacent to the fault plane as bright amplitude reflectors can be traced near the fault plane and thin dramatically upwards in the northeast-direction before being truncated by the overlying mid-Jurassic unconformity (Fig. 9). The boundary between the pre-rift and syn-rift sections is marked by a slight unconformity marked by reflection truncations and differences in seismic amplitude character. I interpret the rift-fill spill across the main, bounding normal fault as the initiation of the sag phase that follows the Phase 2 rift phase (Fig. 9). A thin, relatively undisturbed layer of Louann Salt acts as a cap or seal above the syn-rift (Fig. 9). The southwest-dipping normal fault that represents the up-dip limit of salt tectonics does not penetrate below

the salt and likely detaches onto the base of salt reflectors.

The Moho reflector is also identified directly beneath the AR as shown on Figure 9. In this area, the Moho rises to a depth of approximately 30 km from its full continental thickness of 34-37 km beneath the onshore area of Florida. At a vertical exaggeration of 5 on the seismic line in Figure 9, the Moho appears rises beneath the thinned crust of the AR before returning to a near-horizontal position beneath the less thinned flanks of the AR.

**Figure 9. A.** Uninterpreted northeast-trending seismic dip-line DE-1643 across the Apalachicola rift (location of line shown on map in Figure 5) **B.** Interpreted northeast-trending seismic dip-line illustrating a low-angle normal fault (LANF). The LANF dips around 33° to the northeast and is likely detaching into weaker crust at a depth of 20-22 km. This fault dip is consistent with other LANF-controlled rifts along the east coast of the USA including the Newark Basin that dips at 30° and reactivated Paleozoic thrust faults (Withjack et al., 2013). Deeper stratigraphic units have a shallower dip around 16° with younger units showing even shallower dips. Pre-rift and/or basement reflectors appear to terminate along the approximate base of the syn-rift section. An approximate pre-rift zone of Paleozoic clastics/metasedimentary is interpreted/extended from the nearby FM-252 well that penetrated Orodovician clastic rocks without encountering igneous basement.

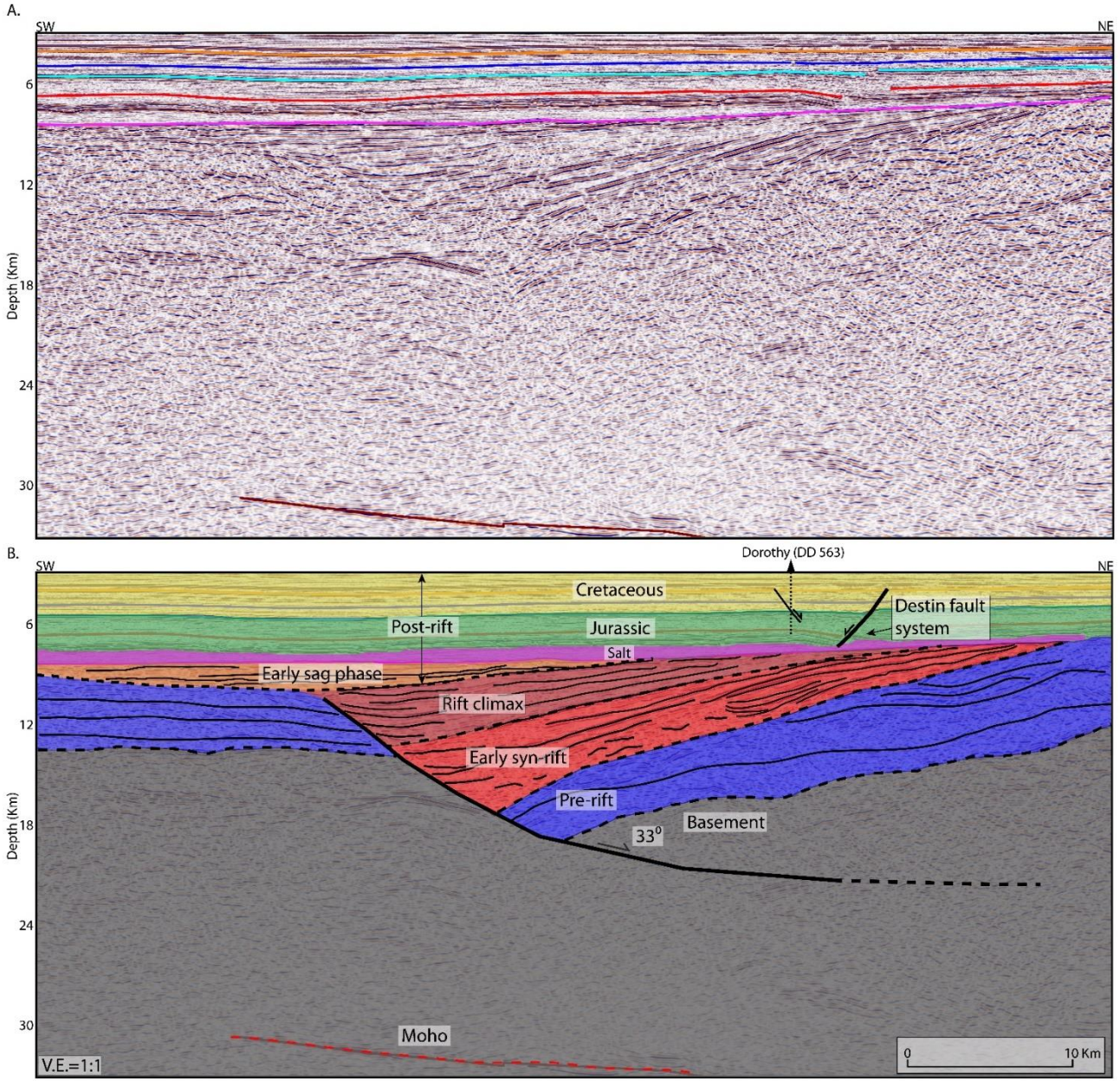
A.
SW
NE
6
12
18
24
30
Depth (Km)
B.
SW
NE
Dorothy (DD 563)
Cretaceous
Post-rift
Jurassic
Destin fault system
Salt
Early sag phase
Rift climax
Early syn-rift
Pre-rift
Basement
33°
Moho
V.E.=1:1
0
10 Km

The easternmost section consists of northeast-dipping LANFs with characteristic pattern of alternating highs and lows as seen on the strike seismic line shown in Figure 10. The westernmost high is more prominent with more pronounced onlaps and thinner, overlying drapes whereas the easternmost high is less pronounced (Fig. 10).

**Figure 10. A.** Uninterpreted northwest-trending seismic strike line DE-380a and DE-380b along the northern section of the Apalachicola rift (location of line shown on map in Figure 5). **B.** Interpreted northwest-trending seismic strike line that also includes the seismic displayed in Figure 4. This figure illustrates intrabasin highs and lows of unlinked half-graben normal faults that create the characteristic pattern of undulating ramps. A similar example from a low-angle fault system occurs in Thailand as shown by Morley (2009).

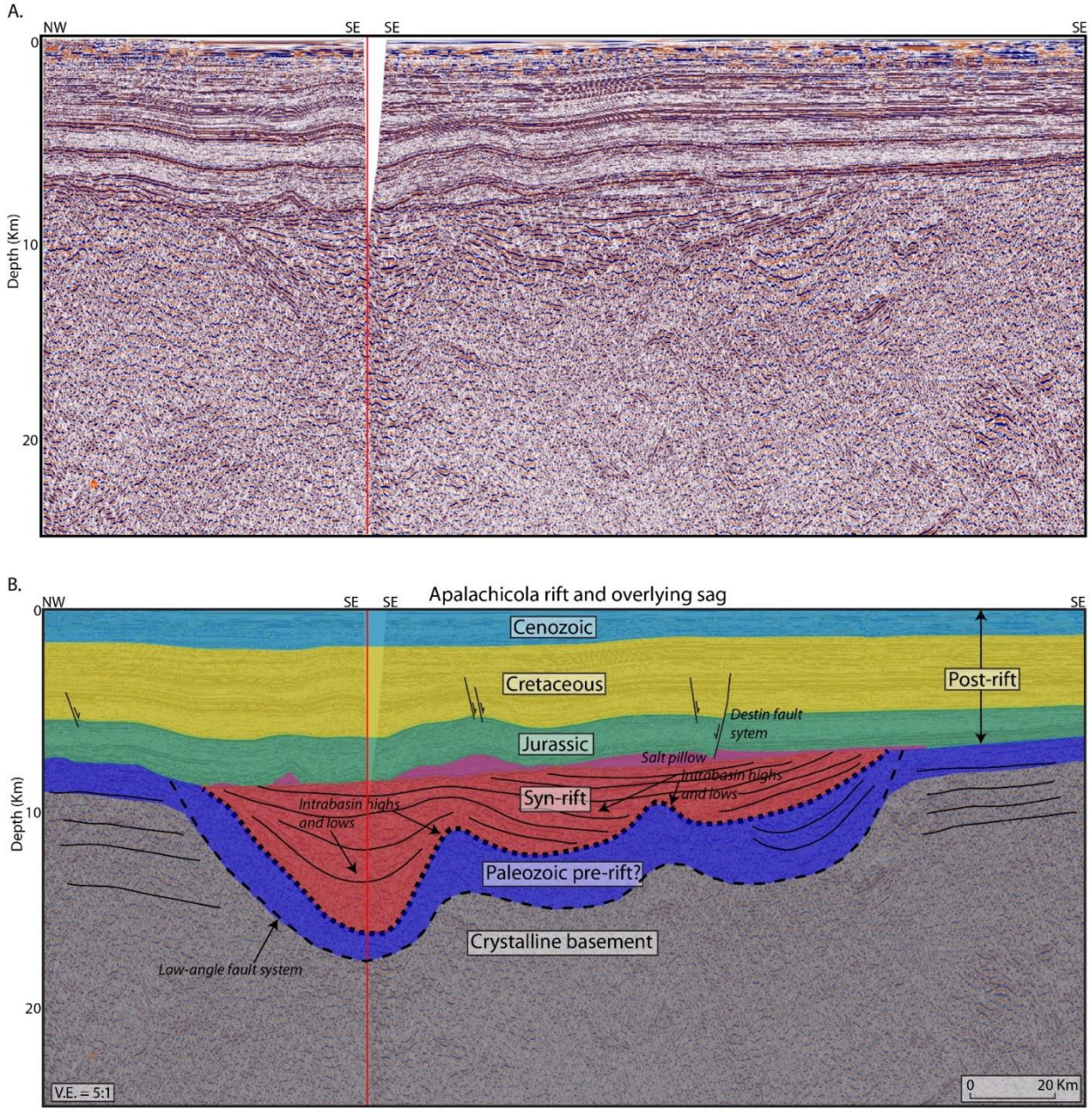
A.
NW
SE
SE
SE
0
10
20
Depth (Km)
B.
Apalachicola rift and overlying sag
NW
SE
SE
SE
0
10
20
Depth (Km)
Cenozoic
Cretaceous
Jurassic
Syn-rift
Paleozoic pre-rift?
Crystalline basement
Post-rift
Destin fault sytem
Salt pillow
Intrabasin highs and lows
Intrabasin highs and lows
Low-angle fault system
V.E. = 5:1
0
20 Km

The western area of the Apalachicola rift contains thicker syn-rift deposits and exhibits more rotation during the rifting process. Figure 11 depicts a 31° north-to-northeast dipping normal fault with a detachment around 24 km in depth. Stratigraphic units in the deepest part of the basin have large dips between 28°-40° indicating a significant amount of rotation associated with this LANF. A bright amplitude reflector is interpreted as the base of the syn-rift and appear to represent the rift-onset unconformity as the surface can be correlated with the Middle Jurassic unconformity. Truncations also mark this interpreted boundary between pre-rift and syn-rift deposits (Fig. 11).

Folds with the basement of the southern area and are interpreted to represent late Paleozoic deformation that may have localized the Triassic-Jurassic LANFs in this area as observed in the Newark graben by Withjack et al. (2002). Significant wedging is also apparent along in this half-graben although the dip of these wedges varies from steeper in the west to shallower in the east (Fig. 11). As discussed by Xiao and Suppe (1992), this along-strike variation in the dips of the wedges may reflect: 1) minor variations in the border fault dip angle or shape of the fault; 2) variations in the total fault slip after the wedge was deposited; 3) variations in the direction of relative particle motion in hanging-wall collapse; 4) the history of sedimentation rate relative to changes in fault slip rate; and 5) compaction effects as discussed.

**Figure 11. A.** Uninterpreted north-trending seismic dip-line DE-533 across the Apalachicola rift. (location of line shown on map in Figure 5). **B.** Interpreted northeast-trending seismic dip-line illustrating a half-graben normal fault dipping 31° to the northeast and with a detachment at a predicted depth of 24 km. Deeper interpreted horizons have higher dips around 28°-40° indicating significant rotation of syn-rift deposits during the rifting process. Fold-like reflections are interpreted towards the north and likely represent Paleozoic compressional features that are inferred to have provided the initial structural weaknesses required to nucleate the low-angle faults.

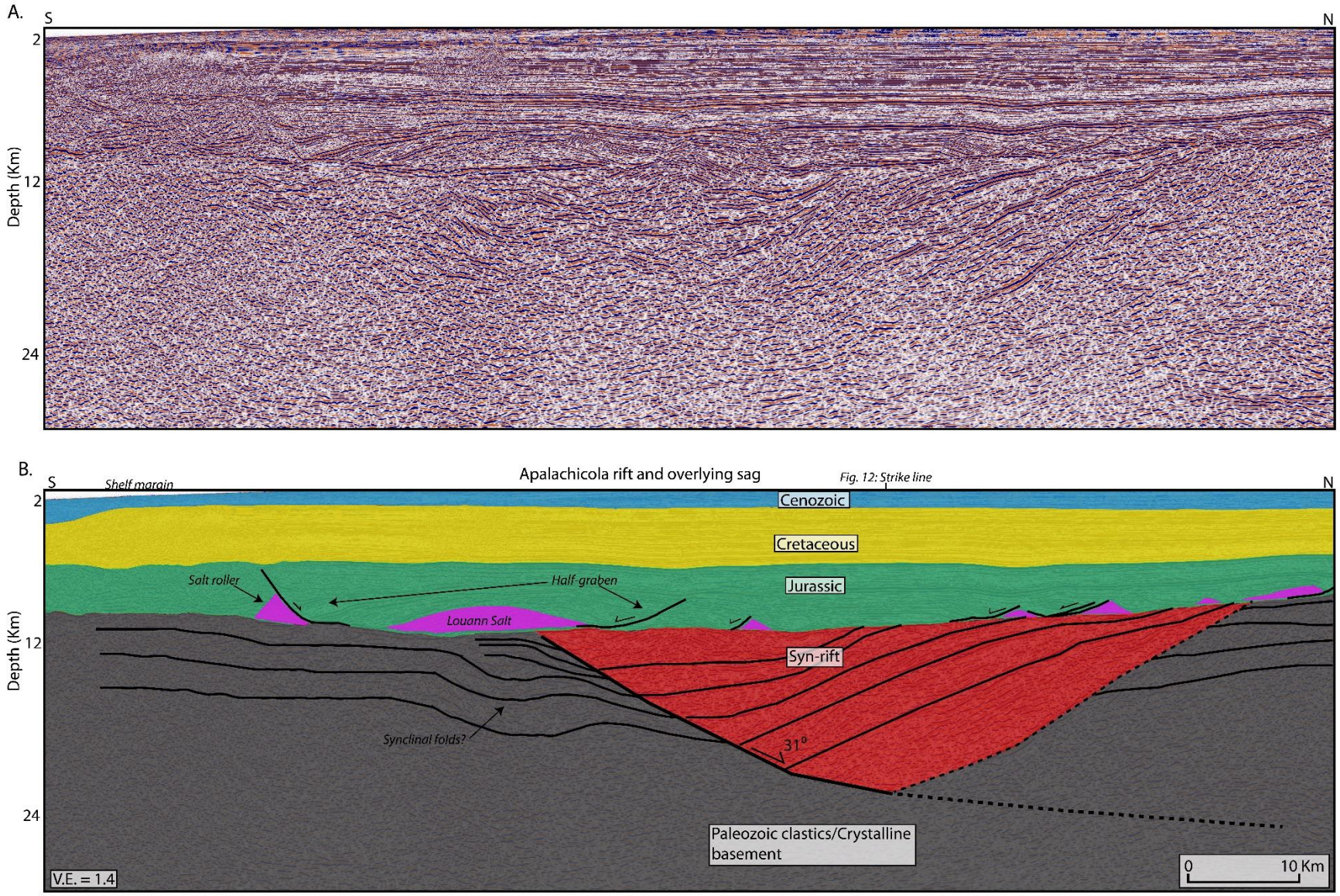
A.
S
N
2
12
24
Depth (Km)
B.
S
Shelf margin
Apalachicola rift and overlying sag
Fig. 12: Strike line
N
2
12
24
Depth (Km)
Cenozoic
Cretaceous
Jurassic
Salt roller
Half-graben
Louann Salt
Syn-rift
Synclinal folds?
31°
Paleozoic clastics/Crystalline basement
V.E. = 1.4
0
10 Km

A strike line shown in Figure 11 through the AR half-graben in section in Figure 12 exhibits a typical bowl-shaped, largely unfaulted syn-rift section. Figure 12B depicts a deep syn-rift section up to 12 km in thickness based on bright amplitude reflections that have northwest- and southeast-dipping orientations. The large unconformity is the rift-onset unconformity that marks the pre-rift-syn-rift transition. Furthermore, the southeast end of the line is dominated by horizontal, continuous reflections whereas the rift comprises gently to steeply dipping reflections and onlapping truncations. Fig. 12 C-E helps illustrate the strike-view geometry of the syn-rift fill as observed on the strike seismic line. On this strike section no alternating intrabasin highs and lows are observed.

**Figure 12. A.** Uninterpreted northwest-trending seismic strike line DE-377 crossing the center of the Apalachicola basin (location of line shown on map in Figure 5). **B.** Interpreted northwest-trending seismic strike that illustrates typical strike view of a half-graben with bowl-shaped geometries, northwest-dipping and southeast-dipping reflections, overlying sag, and onlapping reflections. **C.** Schematic map view of a half-graben with uplifted and down-thrown blocks with seismic line locations indicated. **D.** Schematic transverse or dip view A-A' across the main border normal fault showing the predicted half-graben geometry. Syn-rift sediment is thickening towards the main border normal fault and is progressively thinning and onlapping towards the flexed margin. **E.** Schematic longitudinal or strike view illustrating the bowl-shaped unfaulted basin with the thickest, syn-sedimentary deposits located in the center of the rift near the area of maximum fault displacement. Figures **C-D** are modified from Withjack et al. (2002).

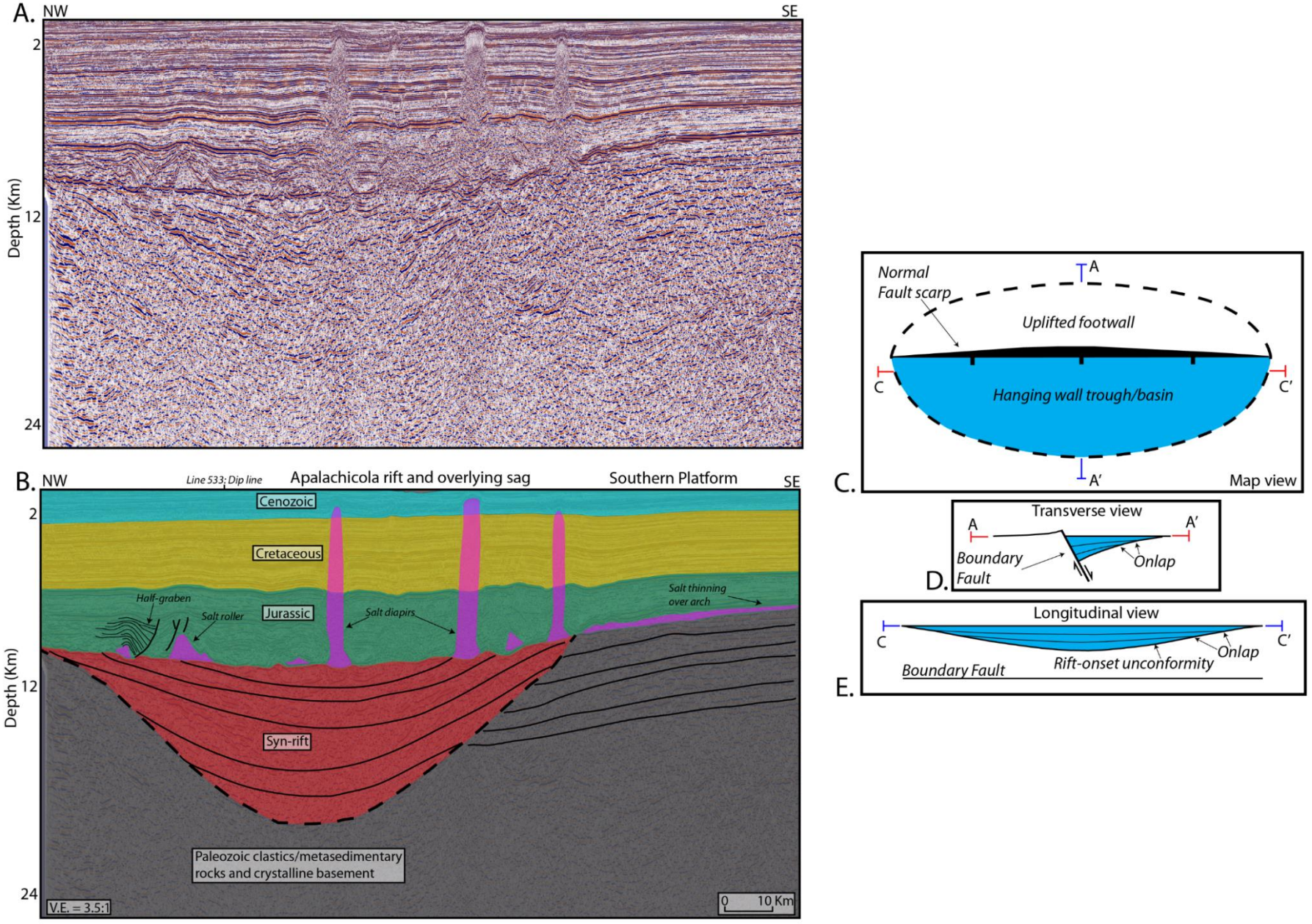
A.
NW
SE
2
12
24
Depth (Km)
B.
NW
Line 533; Dip line
Apalachicola rift and overlying sag
Southern Platform
SE
Cenozoic
Cretaceous
Jurassic
Syn-rift
Half-graben
Salt roller
Salt diapirs
Salt thinning over arch
Paleozoic clastics/metasedimentary rocks and crystalline basement
V.E. = 3.5:1
0 10 Km
C.
Normal Fault scarp
Uplifted footwall
Hanging wall trough/basin
A
A′
C
C′
Map view
D.
Transverse view
Boundary Fault
Onlap
E.
Longitudinal view
Boundary Fault
Rift-onset unconformity
Onlap

### 2.5.2 Structural modeling of half-grabens of the Apalachicola rift

In order to verify the shape of the listric normal faults interpreted from seismic data and to estimate the amount of erosion of both the hanging wall and foot wall during the rifting process, I carried out forward modeling using Structure Solver software for some areas of the AR. Figure 13 illustrates a forward model of the structural evolution of the half-graben shown on the dip seismic section in Figure 9. The results of the modeling shown in Figure 13 predicted a fault angle of 32.7° that required a detachment around the 20-km depth mark in order to be consistent with the observed amount of rotation and tilt involved in the rifting process. This predicted geometry matched the strong observed reflectors of growth strata.

Approximate ages were assigned to the stratigraphic units in the model and based on a recent compilation by Frederick et al. (2020) of published age ranges for the Eagle Mills Formation and Phase 1 rifting (e.g. late Triassic-early Jurassic). The resulting model predicts fault throws up to 8 km for the deepest horizons and around 4-6 km for the youngest syn-rift strata. Modeling also suggests 2.4 km of pre-salt sediment erosion took place at a rate of 193 m/Myr that began in the Toarcian (178 Ma) and ended by the late Early Jurassic before the onset of salt deposition. Although the ages in this model remain uncertain, it's likely that the pre-salt section was significantly eroded for about 12 Ma before being submerged beneath the middle Jurassic sag basin. 2-3 km of predicted erosion for the AR is reasonable when compared to the Newark rift which experienced 2-5 km of erosion based on analytical modeling by Withjack et al. (2013).

**Figure 13. A.** Structural modeling using the Structure Solver software for the seismic profile shown in Figure 9. Location of seismic line shown in Figure 5. Modeling supports LANF dip angle of 32.7° and a predicted, normal detachment around 20 km in depth in order to restore the interpreted to reasonable pre-rift positions. Erosion of around 2-3 km is predicted to have occurred based upon stratigraphic syn-rift truncations along the Middle Jurassic unconformity. This unconformity appears as a relatively smooth angular unconformity across the West Florida Shelf and indicates that significant erosion of presalt strata took place over a period of millions of years (MacRae and Watkins, 1995). The predicted amount of erosion (~2-3 km) is also consistent with erosion estimates (2-5 km) calculated from vitrinite reflectance data in the Newark Basin in the northeastern USA (Withjack et al., 2013). **B.** Forward modeling of the half-graben structural evolution is based on fission-track ages for Phase 1 rifting (late Triassic-early Jurassic). Based on the inferred ages, erosion is predicted to have begun in the Toarcian around 178 Ma with a deposition rate of 193 m/Myr. Waning of rifting is marked by the formation of a late rift, sag spillover phase seen at the top of the main, bounding normal fault with continued presalt deposition based on planar-like stratigraphic units that truncate against the unconformity.

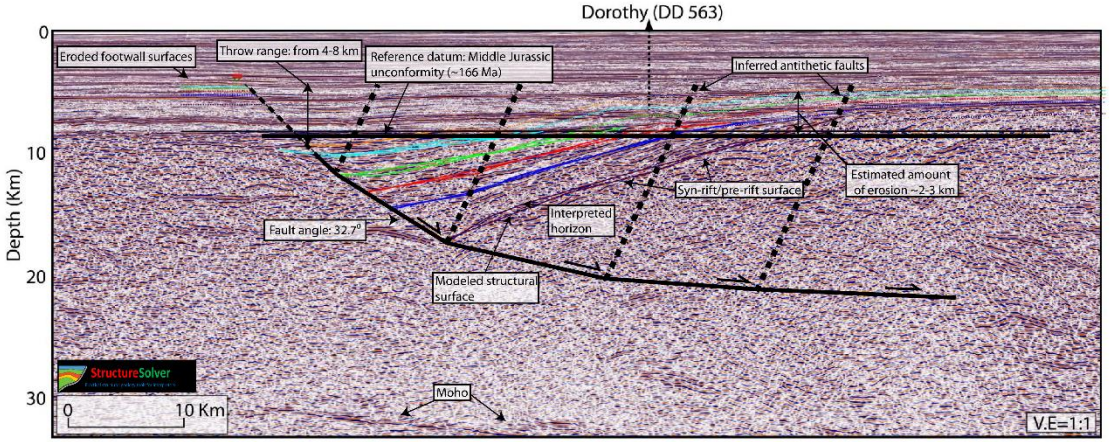
Dorothy (DD 563)
Depth (Km)
0
10
20
30
Eroded footwall surfaces
Throw range: from 4-8 km
Reference datum: Middle Jurassic unconformity (~166 Ma)
Inferred antithetic faults
Estimated amount of erosion ~2-3 km
Syn-rift/pre-rift surface
Interpreted horizon
Fault angle: 32.7°
Modeled structural surface
Moho
StructureSolver
0
10 Km
V.E=1:1

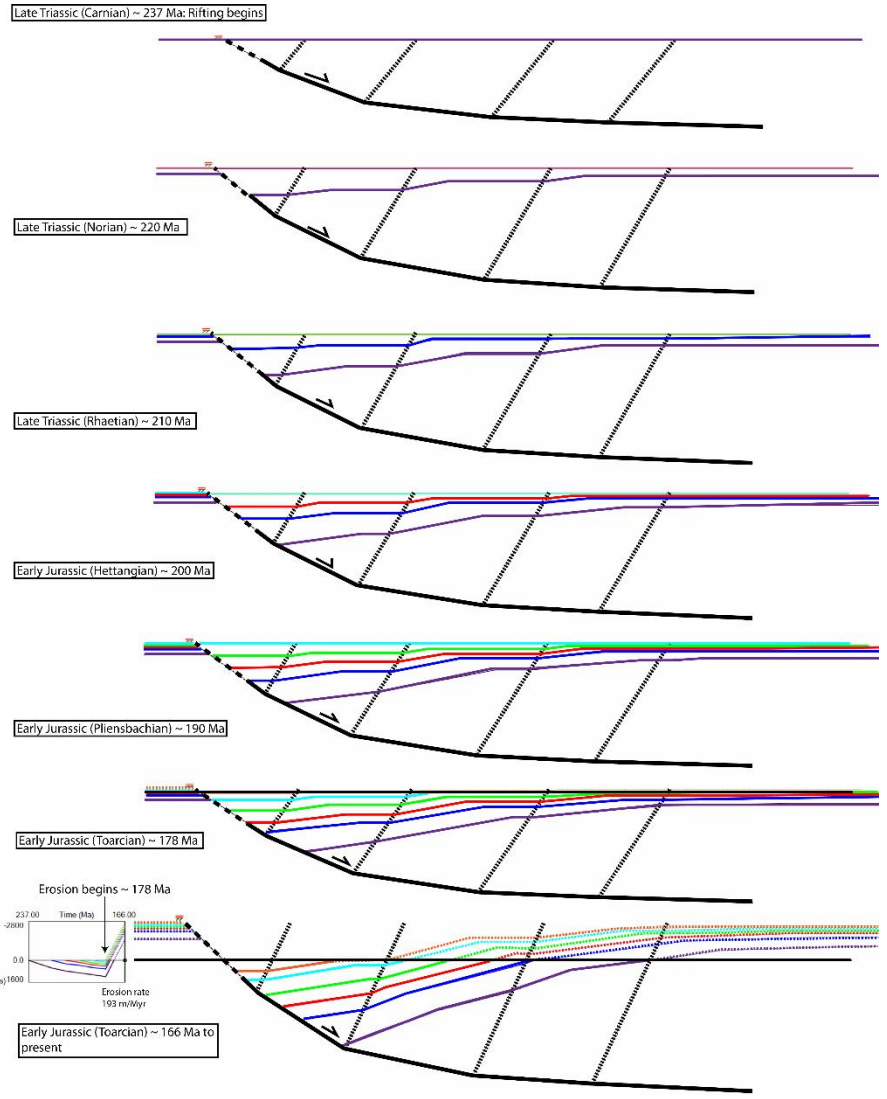
Late Triassic (Carnian) ~ 237 Ma: Rifting begins
Late Triassic (Norian) ~ 220 Ma
Late Triassic (Rhaetian) ~ 210 Ma
Early Jurassic (Hettangian) ~ 200 Ma
Early Jurassic (Pliensbachian) ~ 190 Ma
Early Jurassic (Toarcian) ~ 178 Ma
Erosion begins ~ 178 Ma
237.00
Time (Ma)
166.00
-2800
0.0
1600
Erosion rate
193 m/Myr
Early Jurassic (Toarcian) ~ 166 Ma to present

### 2.5.3 Late Paleozoic structural weaknesses.

The Newark rift along the east coast of North America is a low-angle normal fault half-graben that is proposed to have formed by reactivation of late Paleozoic thrust faults (Withjack et al., 2013). Ratcliffe et al. (1986) analyzed core data from the Newark Basin from the uplifted footwall and determined that the footwall zone contains a zone of extensive mylonites that are observed in seismic data as high-amplitude reflections along the bounding, normal fault. Withjack et al. (2013) concluded that these high-amplitude reflections seen in the Newark rift are reactivated Paleozoic thrust faults that resulted from the Appalachian orogeny.

Although the Apalachicola rift contains half-grabens with similar dip angles, there are no signs of mylonitic features in the seismic data or in nearby well penetrations. In the Florida panhandle, Arden (1974) noted the presence of large synclines in Paleozoic rocks that he inferred were formed after the middle Devonian but prior to Triassic rifting when the area was deeply eroded to a large peneplain. Triassic sediment deposition largely consisted of red beds on top of Silurian-Devonian sandstone-shale sequences and Ordovician quartzite.

Figure 14B shows my reinterpretation of the Elbow Rift feature at the northeastern end of the Tampa Embayment and is shown in map view in Figure 18. The overall elongate trend of the Elbow rift is northwest to southeast so is not in the correct orientation to be an Appalachian shortening-related syncline that would trend northeast to southwest. I re-interpret this feature as a half-graben with a normal fault cutting through the center of the basin and dipping to the northeast (Fig. 14B).

Although the distance from this rift to the Apalachicola rift is around 200 km, the Elbow basin occurs along the same trend as the AR (Fig. 18). Figure 14D illustrates a syncline adjacent to a half-graben in the Apalachicola rift to illustrate the similarity in the geometry of the two structures and from those observed in onshore Florida by Arden (1974).

**Figure 14. A.** Uninterpreted northeast-trending seismic line DE-630 crossing the Elbow rift on the northeastern edge of the Tampa Embayment. Location of seismic line shown on map in Figure 5. **B.** Interpreted northeast-trending seismic line that illustrates a half-graben rift that is parallel with the Apalachicola rift trend and perpendicular to northeastern Paleozoic orogenic activity. **C.** Uninterpreted north-south trending seismic line DE-554 across the Apalachicola rift. Location of seismic line shown on map in Figure 5. **D.** Interpreted north-south trending seismic line illustrating a half-graben adjacent to a syncline. Arden (1974) observed synclines in onshore Florida near the Apalachicola embayment and interpreted them as Paleozoic in origin and containing Silurian to Devonian sediments.

A.

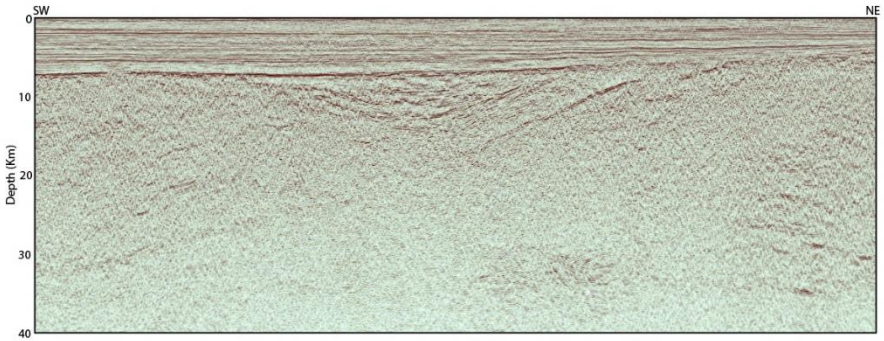
SW
NE
0
10
20
30
40
Depth (Km)

C.

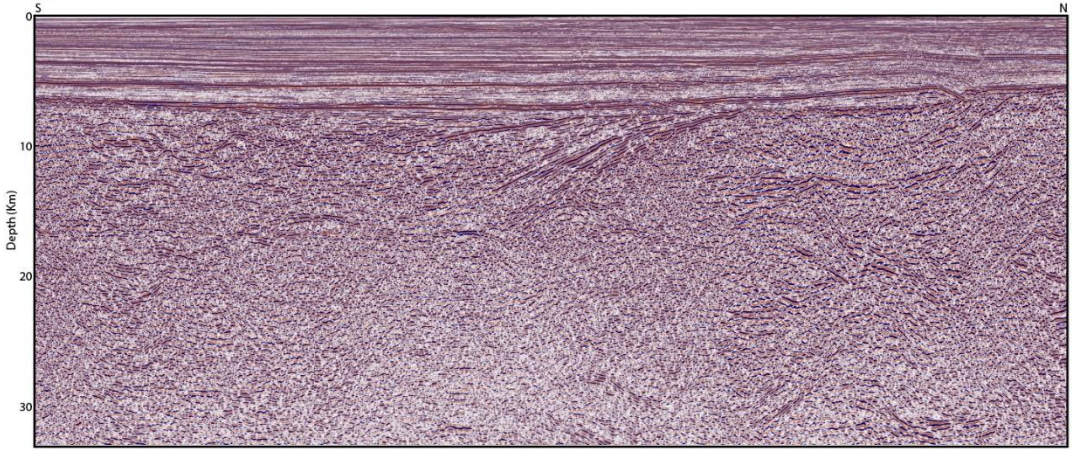
S
N
0
10
20
30
Depth (Km)

B.

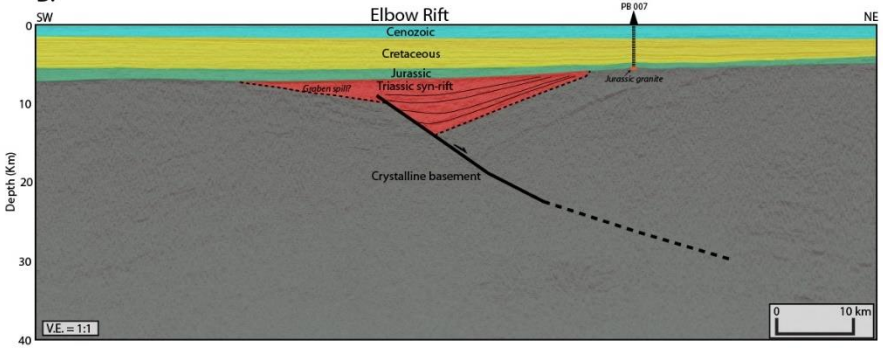
SW
NE
Elbow Rift
PB 007
Cenozoic
Cretaceous
Jurassic
Triassic syn-rift
Graben split
Jurassic granite
Crystalline basement
0
10
20
30
40
Depth (Km)
V.E. = 1:1
0
10 km

D.

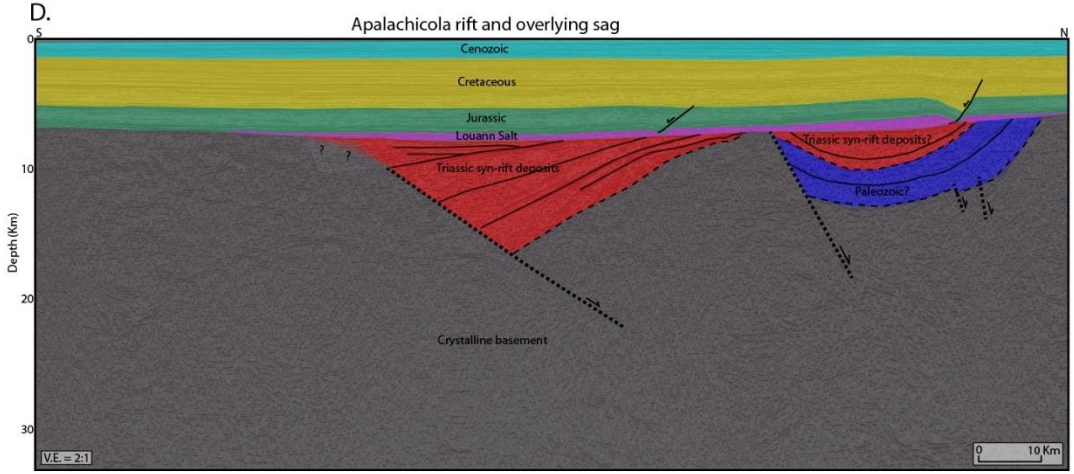
S
N
Apalachicola rift and overlying sag
Cenozoic
Cretaceous
Jurassic
Louann Salt
Triassic syn-rift deposits
Triassic syn-rift deposits?
Paleozoic?
Crystalline basement
0
10
20
30
Depth (Km)
V.E. = 2:1
0
10 Km

## 2.6 Stratigraphy and seismic facies of the pre-salt, Apalachicola rift in the northeastern Gulf of Mexico

### 2.6.1 Well penetrations into pre-salt, syn-rift sections

Figure 15B illustrates an interpreted seismic profile tied to one of the only wells that penetrates up to 2 km of Triassic sedimentary rocks, Paleozoic intrusive rocks, and Precambrian sedimentary rocks (personal communication from Ted Godo, 2020). Beneath the post-rift section, the Sohio (GV 707) well encountered 2760 ft of continental red beds of the Eagle Mills Formation with thick volcaniclastic rocks near the bottom of the interval. Ages were constrained based on an abundance of plant debris and rare pollen and spores. Immediately after this red bed interval, the well encountered around 820 ft of basalt possibly related to early Triassic CAMP age volcanism. The rock types and ages in this well are consistent with other penetrations into Triassic rift zones including the Newark Series along the east coast of North America, the La Boca formation in Mexico, and the Chinle Formation in Colorado, USA (Salvador, 1987; Frederick et al., 2020).

**Figure 15. A.** Uninterpreted northwest-trending seismic lines DE-436 and DE-438 crossing the Sohio GV-707 well that was drilled into syn-rift deposits of the Eagle Mills formation. Location of line is shown on the map in Figure 5. **B.** Interpreted northwest-trending seismic line illustrating Triassic syn-rift deposits and a possible graben filled with Triassic syn-rift sediments reworked from erosion of adjacent Paleozoic rocks. **C.** Interpreted log from the bottom interval of the Sohio well that penetrated up to 2 km of syn-rift sedimentary rocks with interbedded and intruded igneous rocks.

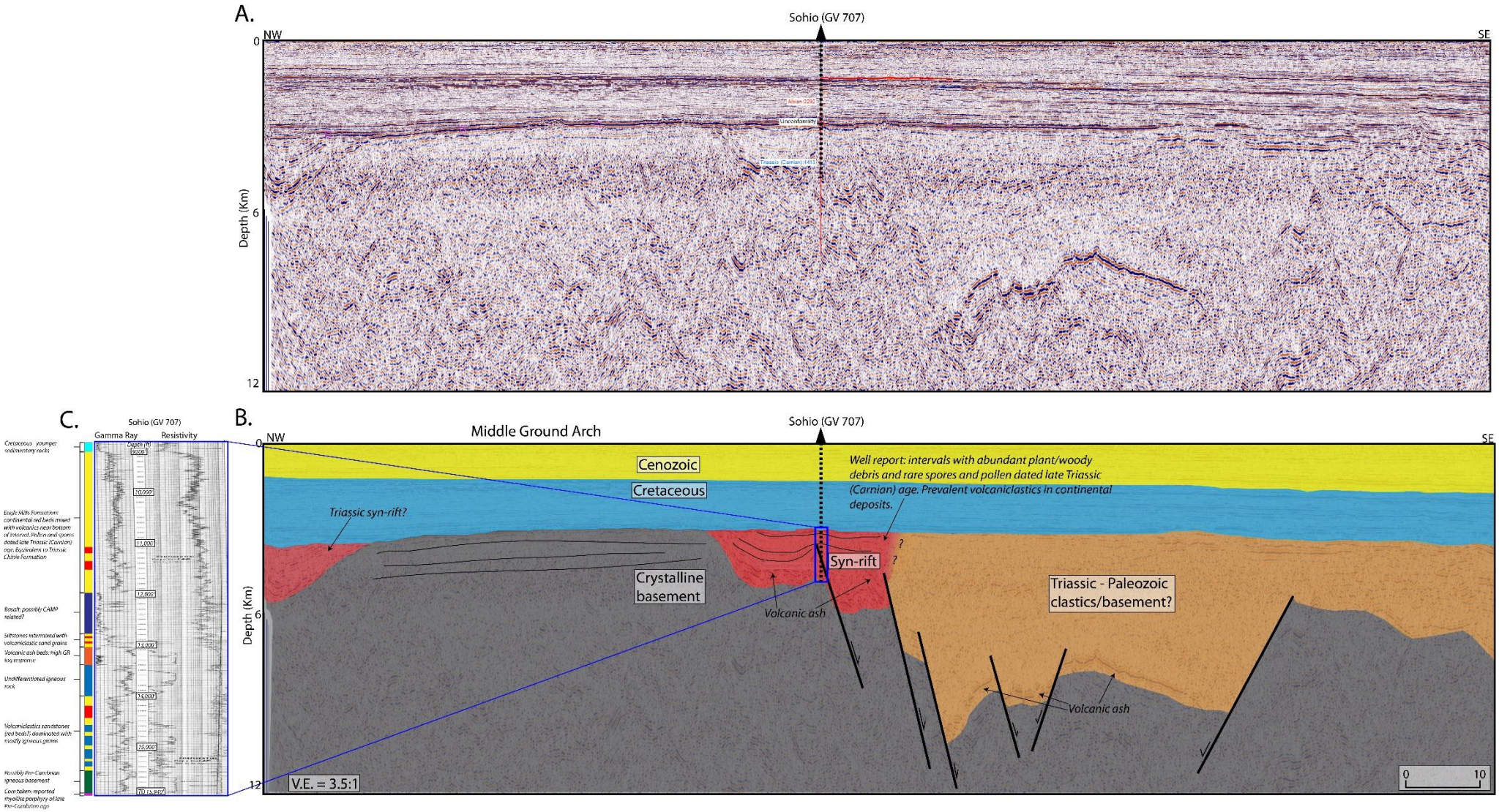
A.
Sohio (GV 707)
NW
SE
0
Depth (Km)
6
12
Unconformity
B.
Middle Ground Arch
Sohio (GV 707)
NW
SE
Cenozoic
Cretaceous
Well report: intervals with abundant plant/woody debris and rare spores and pollen dated late Triassic (Carnian) age. Prevalent volcaniclastics in continental deposits.
Triassic syn-rift?
Syn-rift
Crystalline basement
Volcanic ash
Triassic - Paleozoic clastics/basement?
Volcanic ash
V.E. = 3.5:1
0
10
C.
Sohio (GV 707)
Gamma Ray
Resistivity
Depth (ft)
9,000
10,000
11,000
12,000
13,000
14,000
15,000
TD 15,949'
Cretaceous younger sedimentary rocks
Eagle Mills Formation: continental red beds mixed with volcanics near bottom of interval. Pollen and spores dated late Triassic (Carnian) age. Equivalent to Triassic Chinle Formation
Basalt: possibly CAMP related?
Siltstones intermixed with volcaniclastic sand grains
Volcanic ash beds: high GR log response
Undifferentiated igneous rock
Volcaniclastics sandstones (red beds?) dominated with mostly igneous grains
Possibly Pre-Cambrian igneous basement
Core taken: reported rhyolite porphyry of late Pre-Cambrian age

### 2.6.2 Sedimentation patterns in half-grabens

Normal fault displacement is the main control on the geometry and facies of syn-rift fill. Other factors that affect the facies and lithologies include: 1) the volume of available accommodation space (which is related to basin-margin footwall uplift and/or crustal extension); 2) the lithologies exposed and eroded in the footwall block; 3) the source areas for detrital siliciclastic rocks deposited in the rift; 4) the paleoclimate; and 5) the depths of rift-controlled lakes (Davison and Underhill, 2012; Post and Coleman, 2015).

When subsidence is more rapid than sedimentation in half-grabens, strong onlap of stratigraphic units can occur onto the flexed and unfaulted margin. Alternatively, if subsidence is equal to sedimentation rates, then stratigraphic units can thicken or wedge along the main half-graben boundary fault, onlap pre-rift units, and converge towards the edge of the flexed margin (Withjack et al., 2002; Davison and Underhill, 2012).

The most basic stratigraphic units associated with rifting are the pre-rift, syn-rift, and post-rift packages (Withjack et al., 2002). In the northeast GOM, pre-rift strata are largely characterized by undisturbed planar or nonconvergent, parallel bedded units (Fig. 9). During extension, the syn-rift section is characterized by divergent reflectors that thicken towards the bounding normal fault. Along the bounding fault, the fault scarps and the uplifted footwall block will erode to create a source for coarse-grained alluvial fans and deltas to develop and be distributed along the basin margins. This zone of coarse sedimentation is normally about 5 km in width and can reach up to 4 km in thickness (Davison and Underhill, 2012).

As rifting subsides, stratigraphic onlap onto the divergent reflectors can occur with

sediments deposited as parallel bedded units during the unfaulted sag phase. Underhill and Davison (2012) outline typical lithologies and depositional environments for a continental extensional rift system.

Although a wide variety of depositional environments can exist in non-marine rift basins, two regimes are dominant: fluvial and lacustrine (Withjack et al., 2002). Initial stratigraphic units deposited during the onset of rifting include basal fluvial units dominated by coarse clastic sediment, followed by a transition to deeper water lacustrine sediments (Davison and Underhill, 2012). During lake filling, deltaic, lake shoreline and deep-water lacustrine facies are onlapped by fluvial and alluvial facies (Davison and Underhill, 2012). This stratigraphic succession and architecture produces a "tripartite stratigraphy" that reflects changes in the relative balance between sediment supply, water supply, and accommodation space (Withjack et al., 2002).

### 2.6.3 Seismic facies analysis of the syn-rift fill of the Apalachicola half-grabens

The rift-related facies in the Apalachicola rift remains largely unstudied because insufficient seismic depth penetrations from previous publications restricted the ability to analyze the syn-rift in detail. Additionally, the lack of well-control creates difficulties in assigning lithologies and accurately defining facies. For these reasons, my approach for this study is to construct a seismic facies classification based solely on seismic interpretation and analog models developed by Davison and Underhill (2012) as shown on Figure 16 to help identify features and define depositional environments and lithologies. Seismic reflection parameters - such as configuration, continuity, amplitude, and frequency within the stratigraphic framework of the depositional sequence - were used to help infer the paleoenvironments and lithofacies from the seismic data.

Seismic reflection configurations reveal gross stratification patterns from which depositional processes, erosion, and paleotopography can be interpreted (Bally, 1987). Reflection continuity suggests widespread uniform stratified deposits and the amplitude and frequency provide information on velocity and density contrasts as well as the spacing of beds (Bally, 1987).

**Figure 16.** Seismic facies classification of eight types of syn-rift deposits within the AR based on the methods of seismic character analysis as described by Bally (1987). Location of seismic shown on map in Figure 5. Eight distinctive, seismic stratigraphic features from the syn-rift are described from the seismic lines shown using seismic character traits that include: reflection configuration, continuity, amplitude, and frequency to determine the possible environment of deposition. Except for the inferred coarse-grained, fault-scarp breccias shown on line SF-8, the other seismic facies 1-7 are well stratified and indicative of a finer-grained, fluvial or submarine syn-rift deposit. The observed variability in fault wedging is inferred to reflect variations in the amount of fault activity during their deposition.

| Facies | Seismic example | Interpretation/schematic | Seismic character | Occurrence |
|---|---|---|---|---|
| SF-1 Line 1595 | 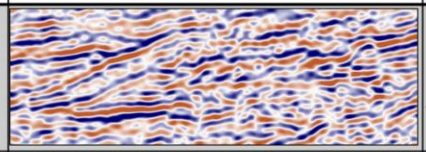 | 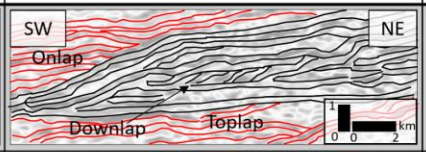 | Semi-continuous to continuous, wavy to chaotic, high frequency reflection package with moderate strength | SW-prograding, possible deltaic-lacustrine sequence that occurs near fault zone in the MRP; high risk interp. |
| SF-2 Line 1595 | 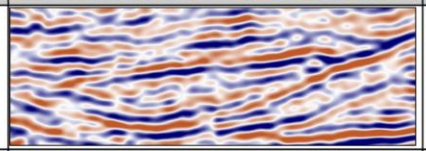 | 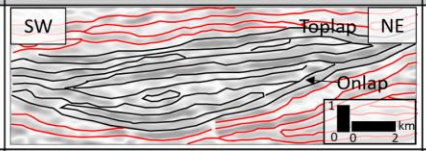 | Semi-continuous to continuous, wavy, subparallel, concave, high frequency reflection package with moderate amplitude strength | Trough/channel fill with onlap truncations, developed adjacent to normal fault, structural origin |
| SF-3 Line 1699 | 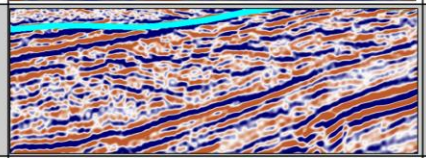 | 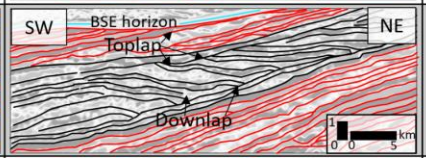 | Semi-continuous to discontinuous, wavy to chaotic reflection package with moderate to high amplitude strength | NE-prograding features with downlap and toplap truncations near BSE, occurs in MRP |
| SF-4 Line 1643 | 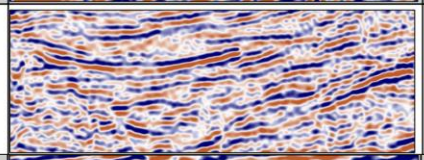 | 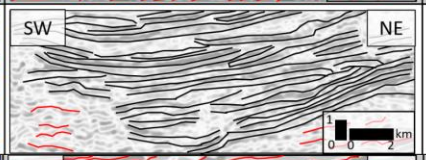 | Semi-continuous, wavy to chaotic, convergent reflections with moderate to high amplitude strength | Occurs along border fault, likely coarse alluvial fan-delta deposits |
| SF-5 Line 1699 | 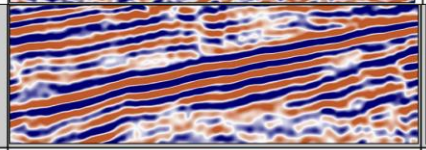 | 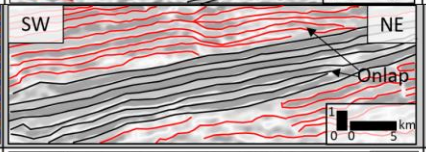 | Continuous, parallel, thick, stacked reflection packages with high amplitude strength | Occurs along pre-rift/syn-rift boundary, likely represents ERP fluvial sequence |
| SF-6 Line 1643 | 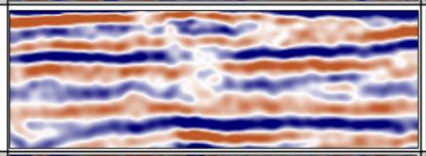 | 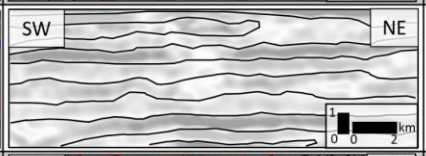 | Semi-continuous, parallel to sub-parallel, low frequency, reflection packages with moderate amplitude strength | Possible shallow water deposition after rifting, sag phase, occurs beneath BSE in LRP |
| SF-7 Line 1643 | 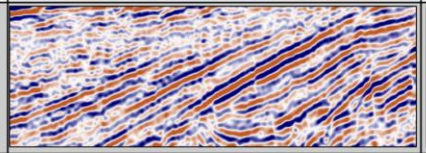 | 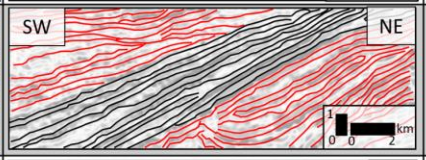 | Semi-continuous, wavy, divergent, dipping reflection packages with intervals of high to low amplitude strength | Widespread wedging units, occurs during ERP and likely represents fluvial deposition |
| SF-8 Line 1595 | 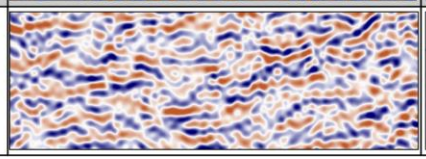 | 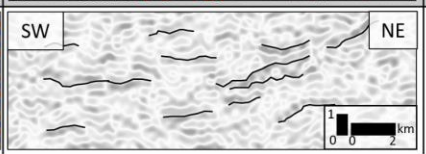 | Discontinuous, contorted, chaotic to wavy reflection packages with variable amplitude strength | Occurs along base of normal fault, likely coarse grained conglomerates/breccia of erosional fill from footwall |

### 2.6.4 Phase 1 syn-rift faulting based on seismic facies variations

The syn-rift section of the AR can be divided into three main sequences based on seismic character. Figure 17 illustrates the observable seismic facies in the Apalachicola rift as well as incorporates a schematic of typical facies and sedimentation patterns in continental rifts. The figure also takes into account the nearby lithology of the Eagle Mills Formation (Arden, 1974). Bright amplitude, continuous, low to high frequency, divergent reflections generally characterize the base of the syn-rift. Noticeable wedging occurs near the bounding normal fault and likely records the early fluvial phase of the syn-rift wedge (Davison and Underhill, 2012).

A similar type of LANF-controlled, syn-rift fill occurs along the boundary between Paleozoic strata and basement in the Newark basin (Withjack et al., 2013). The mid-rift phase is characterized by moderate to high amplitude, semi-continuous reflections along the border fault and moderate to low amplitude, discontinuous, convergent reflections towards the mid-Jurassic unconformity in the northeast-direction (Figs. 16, 17). This zone near the border fault likely represents alluvial fans and deltas prograding out into the basin followed by a facies change to finer material of a lacustrine environment.

The late-rift phase is characterized by moderate to high amplitude, semi-continuous to continuous, semi-parallel, high-frequency reflections occasionally top lap against the mid-Jurassic unconformity and onlap the mid-rift phase units (Figs. 16, 17). The semi-parallel nature of the reflections suggests near-uniform rates of deposition are likely of fluvial origin. The final, lacustrine-fluvial transition requires that faulting slows considerably or even ceases (Withjack et al., 2002; Davison and Underhill, 2012).

**Figure 17.** Inferred seismic stratigraphic facies in an idealized, continental, half-graben modified from Burg (2018), Davison and Underhill (2012), observations from other syn-rift areas of the Gulf Coast region that include well Sake #2 (Frederick et al., 2020), and from my own observations from nearby well penetrations such as Sohio GV-707 well (Fig. 15). Along the main, border nomal fault, coarse deposits of erosional fill from the uplifted footwall block are expected and are expressed as chaotic reflectors that are inferred as alluvial fan deposits. The syn-rift contains noticeable bright amplitude diverging reflections that I infer as an early rift phase that is dominated by deposition of fluvial sandstones and red-green oxic shale and volcaniclastics rocks. The mid-rift to late-rift phase is inferred to be dominated by alluvial fans and channels near the main border normal fault. The thick section of low-amplitude reflections is inferred to be a homogenous layer likely of red bed origin. After the cessation of rifting, continued deposition is evident in the form of planar onlapping and truncated reflections inferred to represent an early sag phase with fluvial sandstone, siltstone, and shale. Inferred basaltic dikes and sills are depicted based on the abundance of well records from the Eagle Mills formation that contain intrusions and volcaniclastic sedimentary rocks dated as young as early Jurassic.

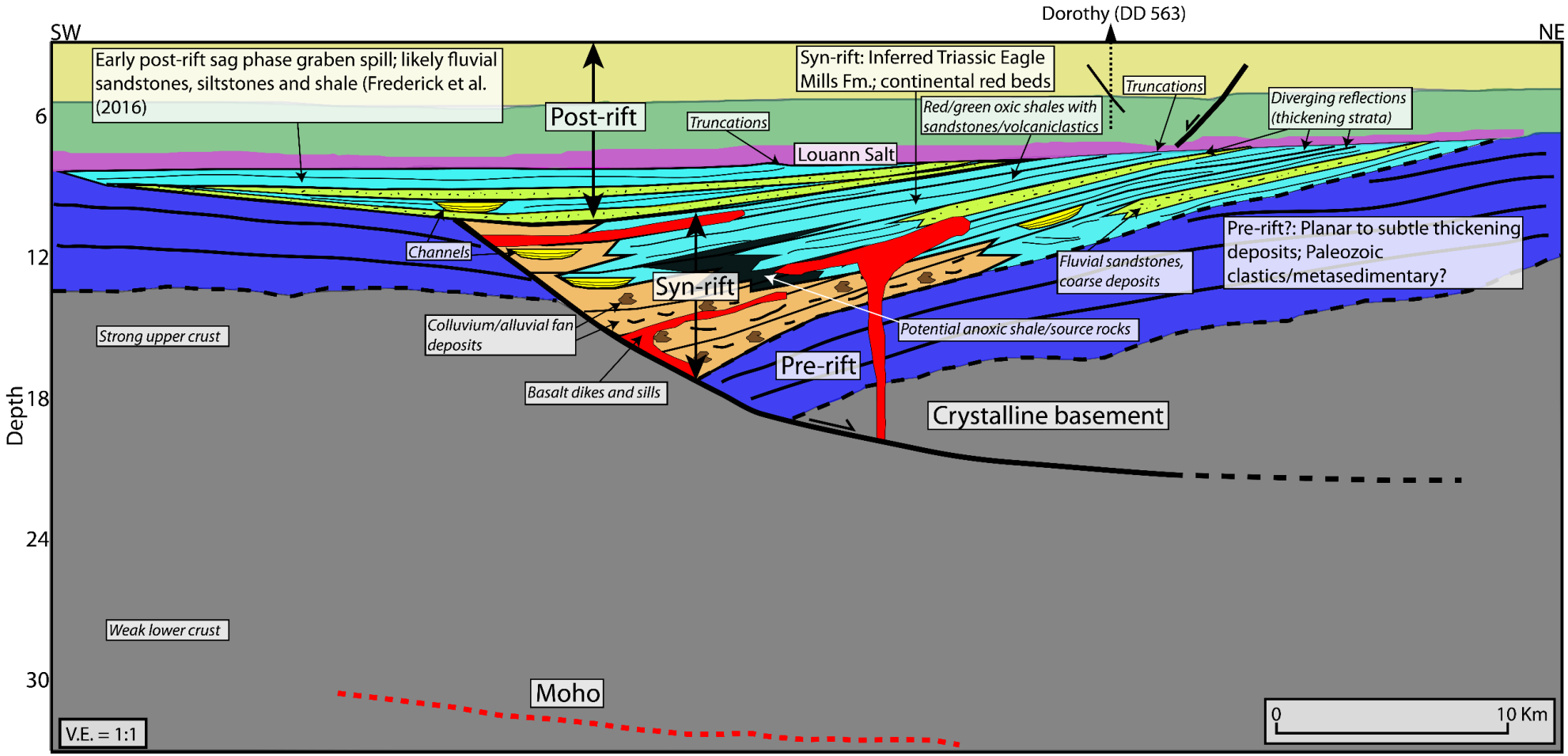
SW
NE
Dorothy (DD 563)
Early post-rift sag phase graben spill; likely fluvial sandstones, siltstones and shale (Frederick et al. (2016)
Post-rift
Truncations
Syn-rift: Inferred Triassic Eagle Mills Fm.; continental red beds
Red/green oxic shales with sandstones/volcaniclastics
Truncations
Diverging reflections (thickening strata)
Louann Salt
Channels
Syn-rift
Fluvial sandstones, coarse deposits
Pre-rift?: Planar to subtle thickening deposits; Paleozoic clastics/metasedimentary?
Strong upper crust
Colluvium/alluvial fan deposits
Potential anoxic shale/source rocks
Pre-rift
Basalt dikes and sills
Crystalline basement
Depth
6
12
18
24
30
Weak lower crust
Moho
V.E. = 1:1
0
10 Km

## 2.7 Discussion

### 2.7.1 Influence of orogenic inheritance on the formation of LANFs

Different structural mechanisms and preexisting, basement structural fabrics can result in the development of LANF's as described by Morley (1989) using LANF examples from Thailand. One model for the formation of LANFs at rifted margins invokes reactivation and normal reversal along low-angle thrust faults that formed during a previous, orogenic shortening event (Withjack et al., 2002; 2013; Morley, 2009). Examples of LANFs that formed along reactivated thrusts include: 1) the Newark, Fundy and Jeanne d'Arc basins along the eastern margin of North America (Withjack et al., 2002, 2013), 2) the Lokichar fault in the southern Turkana area of the East African rift zone in Kenya (Morley, 1989; Morley, 2009); 3) the Torlesse accretionary wedge in New Zealand (Morley, 2009); 4) the Chiang Mai and Phitsanulok basins in Thailand (Morley, 2009); and 5) the Basin and Range province in the western USA (Morley, 2009).

As previously discussed, the Newark rift basin was controlled by a LANF with a fault zone characterized on a 2D seismic line by a series of high-amplitude, planar reflections that correspond to surface outcrops of mylonitic rocks and a 30° dip to the southeast (Withjack et al., 2002; 2013). I propose a similar thrust and fold reactivation mechanism for the origin for LANFs of the Apalachicola rift as supported by the presence of orogenic faults and folds observed in the Apalachicola rift, along the West Florida Shelf, and in onshore Florida (Arden, 1974; Applegate and Lloyd, 1985). This type of inverted, low-angle thrust faults and its similar Appalachian orogenic setting support the application of the Type 2 rift-basin structural style of Withjack et al. (2002) to the Apalachicola rift.

### 2.7.2 Crustal setting of the AR rift zone

The location of the west-northwest-trending Apalachicola-Elbow rifts relative to the shelf edge and deep central GOM basin indicates is role forming the intermediate thickness, continental crust that is shown on Figure 1. This 300-km-long zone of normal faults roughly follows the 40 km crustal thickness line that separates zones of contrasting morphology between the extended crust to the southwest and unextended crust of normal thickness to the northeast as seen in onshore Florida and along the West Florida Shelf (Osmundsen and Péron-Pinvidic, 2018). This transition zone that the Apalachicola rift and Elbow rift lie in has previously been modeled to have beta stretch factors between $\beta$=1.5 near the Florida shoreline and $\beta$ =3 along the West Florida Shelf break using a passive margin model (Dunbar and Sawyer, 1987).

### 2.7.3 Controls on syn-rift depocenters and erosion in LANF settings

In a regional strike view of the eastern-most Apalachicola rift, intrabasin-highs are interpreted with adjacent troughs containing stratigraphic units that thin and onlap onto these highs (Fig. 4). As seen in seismic in the LANF-bounded Suphan Buri Basin of Thailand by Morley (2009), similar folds to those seen in the Apalachicola rift are observed with one or more of troughs separated by intra-basin highs that are controlled by border faults with similar dip directions but with variable fault displacements (Withjack et al., 2002; Morley, 2009). In terms of basin-filling models, deep lakes with potentially thick, lacustrine source rocks can only form when high relief is produced by significant footwall uplift as well as the formation of transfer zones (intra-basin highs) between the normal faults.

Considering the lack of well control in the Apalachicola rift, estimates for the amount of erosion of its syn-rift remains poorly known. However, nearby analogs of the Newark basin and

surrounding basins may provide useful insights for erosion affecting the Apalachicola rift. As seen along the eastern margin of North America, syn-rift stratigraphic units are truncated by an angular unconformity overlying the hanging wall block indicating a period time marked by exposed strata and subsequent erosion (Withjack et al., 2002; Morley, 2009).

On the footwall block, restorations using Structure Solver as shown in Figure 9, shows that a small, fluvial sag basin appears to truncate the controlling listric normal fault. Some erosion of the footwall block is required for LANFs because of the amount of rotation and uplift of the footwall block. Erosional estimates for the Newark graben were carried out by Withjack et al. (2013) using seismic, field, core, borehole and vitrinite-reflectance data that allowed the creation of a contour map illustrating calculated amounts of erosion for both the footwall and hanging wall blocks. Their findings revealed that up to 6 km of syn-rift were eroded and was also accompanied by intra-basin faulting, tilting and folding of syn-rift strata.

### 2.7.4 Control on LANF's on stratigraphy and petroleum systems

Half-graben deposits generally exhibit a tripartite stratigraphic order that include: 1) **fluvial-dominated sediments** that characterize the early stages of rifting; 2) **deltaic-lacustrine settings** that form as the basin depth increases; and 3) **a transition back to fluvial deposition** as rifting ends (Withjack et al., 2002; Davison and Underhill, 2012) (Figure 17). Morley (1989) contrasts the syn-rift stratigraphy resulting from deposition along more steeply-dipping normal faults compared with more gently-dipping normal faults of the East African rift systems. Most of the LANFs identified in this study exhibit relatively smaller vertical displacement ranging up to 12 km as compared to the overall horizontal displacement that averages about 30 km.

LANF's are generally associated with smaller values of syn-rift thickness, although

LANF's that penetrate to greater crustal depths (generally > 15 km) show greater amounts of subsidence (Morley, 1989). This relationship is seen for the westernmost of the Apalachicola half-grabens that show depths of detachment down to depths of 20 km and show corresponding greater thicknesses of their syn-rift fill up to 7.5 km (Figure 8F).

LANF's are more prone to periodic lacustrine conditions but deeper detachments faults are a likely cause for an increase in subsidence and prolonged lacustrine conditions as observed in the Triassic Newark basin where the majority of its syn-rift fill consists of lacustrine sedimentation characterized by gray and black shale with interbedded, coal beds (Withjack et al., 2013).

The Newark supergroup and related rift basins along eastern North America have many documented oil and gas shows but no producing well has been completed (Schultz, 1988). A more recent USGS report (Milici et al., 2012) assessed several of these rift basins and determined kerogen content from these source rocks generally consists of vascular plants and algae material and were assigned a mean estimate of 3.8 bcf of gas and 135 million barrels of natural gas liquids.

In onshore Alabama ~200 km away from my northeast GOM study area, at least seventeen wells have drilled into the Triassic sediments of the Eagle Mills Formation and encountered red beds, sandstones, and conglomerates with intrusive mafic rocks consisting of basalt and diabase dikes and sills (Raymond, 1989). Similarly, igneous rocks such as basaltic lava flows, diabase sheets and dikes in the Newark basin are associated with CAMP (Central Atlantic Magmatic Province) which occurred during the latest Triassic and early Jurassic and can also occur as widespread sills (Withjack et al., 2013). In the South Georgia Rift and in the

offshore half-graben penetrated by Sohio GV-707, continental red beds mixed with volcaniclastics are also interpreted (Applegate and Lloyd, 1985; Raymond, 1989; Christenson, 1990; Godo, 2017). Considering the many high-amplitude, widespread and continuous reflectors present in the Apalachicola rift, it's likely that these strong reflectors could be associated with volcanic sills emplaced during rifting. Contact metamorphism resulting in small garnet crystallizations in a limestone unit within the Eagle Mills Formation was recorded from a well in Alabama (Raymond, 1989).

Given my interpretations of Apalachicola syn-rift sedimentary fill and the generalized, tripartite stratigraphic succession of half-grabens known from other areas like the East African rifts (Fig. 17), the potential for source rock-rich lacustrine settings may exist in the deeply-buried, syn-rift deposits of the northeastern GOM. However, the depositional environment and age of syn-rift sedimentary rocks the around the Triassic-Jurassic GOM by previous workers like Salvador (1987) consists of only continental red beds and volcaniclastics collectively known as the Eagle Mills Formation that appear unlikely to contain high-quality source rocks. Although no source rock has been previously documented from inferred Triassic grabens around the circum-GOM, analyzing global half-grabens with proven potential could aid in determining the GOM potential especially with: 1) the lack of confident Triassic paleogeographic maps; 2) no documented oil seeps or slicks; 3) the lack of a significant number of Triassic well penetrations in offshore GOM; and 4) the many unknowns related to thermal history.

The Lokichar half-graben in the East African rift zone of Kenya contains two proven Cenozoic plays and a possible deep Cretaceous play all derived from early to mid-rift lacustrine source rocks of Eocene and possible Cretaceous age (Loperot and Lokhone shale units) (Neumaier and Mouli-Castillo, 2014). Migration pathways exist both in the up-dip margin

towards the flexed but unfaulted margin as well as upwards along the main, bounding normal fault.

Optimal thermal maturity and transformation ratios are a critical factor for the Lokichar rift as seen for the mature source rocks present in the deepest parts of basin. For the northeastern GOM, the overlying Louann Salt may act to lower heat flow of deeply buried source rocks and additional provide a strong seal for the many potential reservoirs within the underlying eroded and truncated strata (Fig. 17). Yallup (2019) conducted a 2D basin model in the Sureste basin in the southwestern corner of the Gulf of Mexico and revealed that the deeply-buried pre-salt plays are largely within the gas-overmature window. However, Yallup (2019) also noted that the decrease in the thick overburden observed in the study area could provide more optimal thermal maturity conditions.

### 2.7.5 GOM rift phases and their relation to models of two phase GOM opening

The Apalachicola rift (AR) was considered by previous workers as a part of a Triassic-early Jurassic rifted zone formed during the Triassic-early Jurassic stage of the northwest to southeast GOM opening (Martin, 1978; Salvador, 1987; MacRae and Watkins, 1995; and Hunter, 2014) (Fig 1). Eddy et al. (2014) first pointed out that two phases of rifting in the GOM: an earlier, northwest to southeast Phase 1 rifting from late Triassic to early Jurassic and a later, more north-south opening related to extension linked to the counter-clockwise rotation of the Yucatan block (Nguyen and Mann, 2016) (Fig. 1).

The AR has been interpreted as the southwestward, offshore continuation of the onshore South Georgia rift in the southeastern USA and represents the southern terminus of northeast-trending rifts that extend ~780 km along the eastern margin of North America (Clendenin, 2013;

Godo, 2017) (Fig. 1). The South Georgia Rift is a complex series of grabens and half-grabens that trend in a general northeast direction and are occasionally offset by northwest-trending onshore lineaments (Raymond, 1989) (Fig. 1). Because the west-northwest-trending Apalachicola rifts and the parallel Elbow rift 200 km to the southeast (Fig. 1, Fig. 14) are oriented orthogonal and appear to crosscut rifts of the South Georgia rift, I interpret the AR to be relatively younger in age than the northeastern rifts and orogenic fabric that the AR-Elbow rift truncates (Fig.1).

The west-northwest-trending AR and Elbow rifts are colinear with the Florida Lineament as defined by Christenson (1990) (Figs. 2, 18). For this reason, I propose that this rift trend defines the Florida Lineament (at least in its western area) and is an early phase of the late Jurassic Phase 2, Yucatan block-related rifting as proposed by Eddy et al. (2014) (Fig. 19). The later phase of this Phase 2 rotation of the Yucatan block is recorded by the marginal rifts that border the late Jurassic, oceanic crust that underlies the eastern GOM (Lin et al., 2019) (Figs. 1A, B, 18). These earlier Phase 2 basins of the AR and Elbow rift are 200 km from the edge of oceanic crust beneath the deep, central GOM and therefore may have represented a protracted rifting stage that eventually produced enough crustal thinning to lead to the formation of oceanic crust in the deep, central GOM (Fig. 18A, B; 19).

**Figure 18. A.** Merged Bouguer gravity map modified from Bain et al. (2019) for the eastern GOM showing: 1) gravity high trend for early Phase 2 rifts of the AR-Elbow trend shown in white; 2) later Phase 2 rifts adjacent to the oceanic crust in the deep GOM are also shown in white; and 3) and the continent-ocean boundary from Nguyen and Mann (2016) is shown in yellow. The east-west to southeast trend of the early Phase 1, AR-Elbow rift trend is orthogonal to and crosscuts the older, northeast-trending Phase 1 trend and Paleozoic orogenic trends beneath Florida and the West Florida Shelf. The trend of the Florida Lineament is shown as the zone between the dashed yellow lines and coincides with the approximate boundary between the northeast, Phase 1 rift trend and parallel orogenic trends and the younger Phase 2 trend of the AR and Elbow rift. **B.** Total magnetic intensity anomaly map for the eastern GOM from Lin (2018) that further illustrates the crosscutting trend of the early Phase 1 Apalachicola and Elbow rifts. Both rifts are represented by the elongate trends of magnetic highs. The Tampa Embayment exhibits a ~40-km, left-lateral offset from the older Paleozoic Suwannee Basin in the north as defined by a prominent magnetic low and illustrated by left-lateral offset distances in kms.

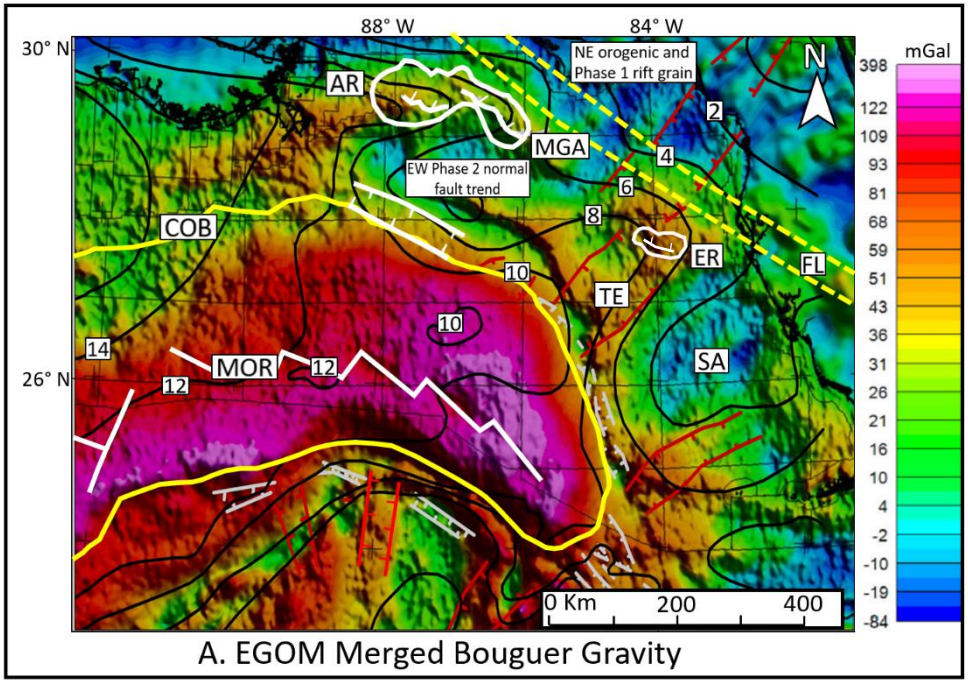


A. EGOM Merged Bouguer Gravity

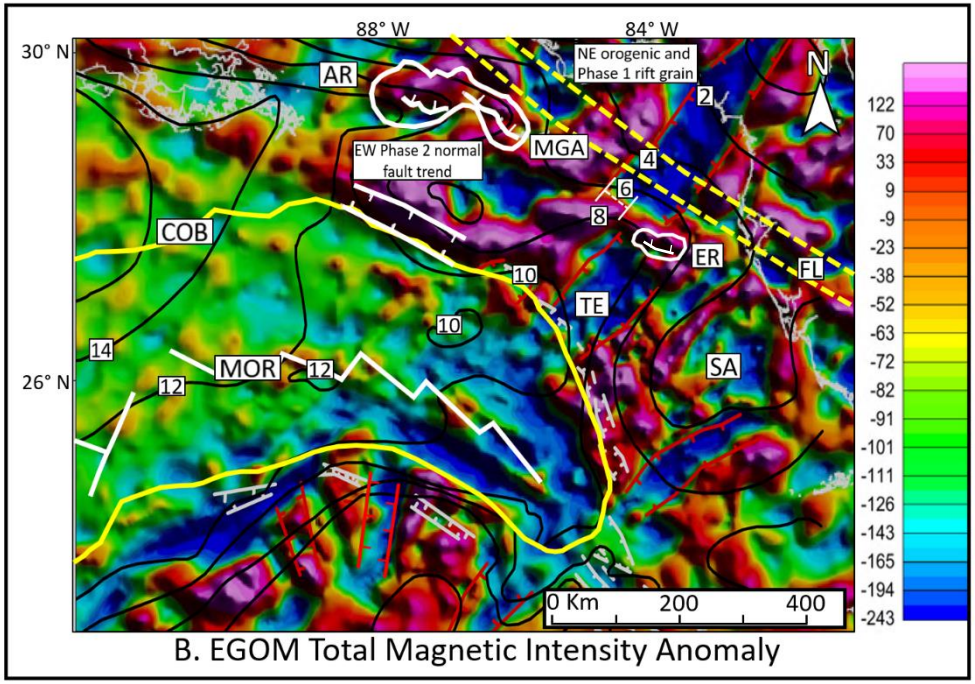


B. EGOM Total Magnetic Intensity Anomaly

In summary, I propose that the cross-cutting nature of the Apalachicola rift and the Elbow rift with the SGR trend as well as the synchronous northwest-orientation of these rifts leads to a possible rift extension northward into the onshore portions of Alabama along the thick/transitional crust boundary as depicted in Figure 18. This west-northwest crustal trend can be projected to connect with the Texas-Louisiana-Arkansas rift trend as described by Salvador (1991).

**Figure. 19.** Plate reconstruction for the Gulf of Mexico modified from Lin (2018). **A.** Late Paleozoic collision resulting in the formation of Pangea that had ceased by the Permian. **B.** Initiation of Phase 1 GOM rifting during the late Triassic to early Jurassic. **C.** By the end of the Phase 1 rifting, many northeast-trending faults are opened as well as the early Phase 2 Apalachicola Rift which cross-cuts the onshore older northeast-trending rifts. Additionally, the proposed north-northwest onshore continuation of AR aligns with rifts identified in the Texas, Louisiana and Arkansas. **D.** Post-Phase 1 salt deposition fills the overlying sag basin during the middle Jurassic. **E.** Phase 2 GOM rifting and oceanic spreading accompanies counter-clockwise rotation of the Yucatan block. **F.** Phase 2 rifting, spreading, and rotating ends during the earliest Cretaceous.

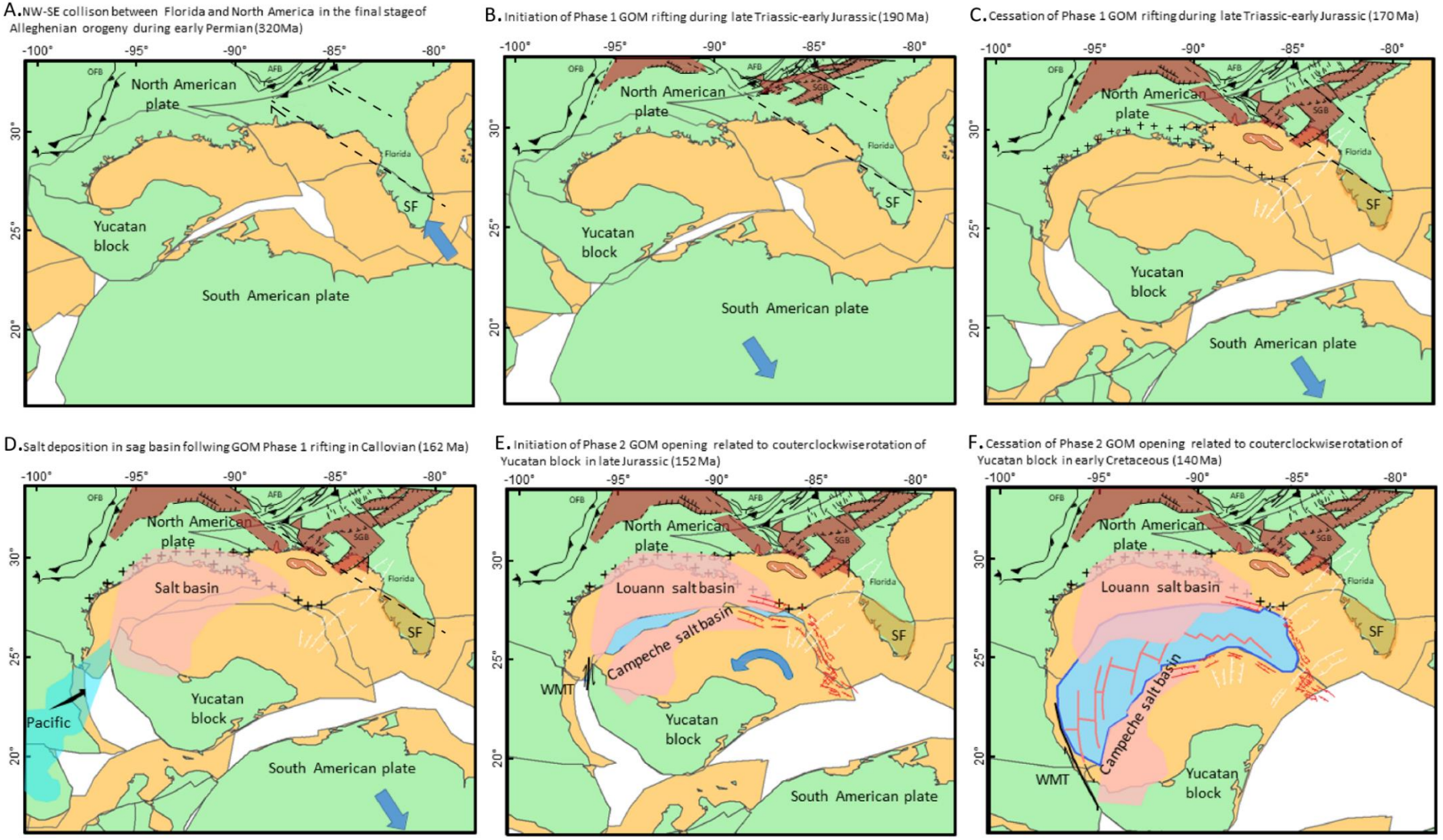
A. NW-SE collison between Florida and North America in the final stage of Alleghenian orogeny during early Permian (320Ma)
B. Initiation of Phase 1 GOM rifting during late Triassic-early Jurassic (190 Ma)
C. Cessation of Phase 1 GOM rifting during late Triassic-early Jurassic (170 Ma)
D. Salt deposition in sag basin follwing GOM Phase 1 rifting in Callovian (162 Ma)
E. Initiation of Phase 2 GOM opening related to couterclockwise rotation of Yucatan block in late Jurassic (152 Ma)
F. Cessation of Phase 2 GOM opening related to couterclockwise rotation of Yucatan block in early Cretaceous (140 Ma)
-100°
-95°
-90°
-85°
-80°
30°
25°
20°
OFB
AFB
SGB
North American plate
Florida
SF
Yucatan block
South American plate
Salt basin
Pacific
Louann salt basin
Campeche salt basin
WMT

## 2.8 Conclusions

1. The Mesozoic Apalachicola rift (AR) is controlled by two major *en echelon* half-graben normal faults that trend in a west-to-northwest direction and exhibit low to moderate dips (28°-40°) to the north and northeast. The half-grabens are filled by 5-8 km of undrilled, clastic and possibly volcanic or intrusive rocks. The AR along with the Elbow rift 200 km to the southeast comprise a 300-km-long, northwest-trending line of rifts that form a major tectonic boundary that truncates northeast-trending basement fabric that underlies the West Florida platform and the mainland of Florida.

2. The AR-Elbow northwest rift trend also truncates Phase 1 northeast-trending faults that bound Phase 1 rifts of inferred late Triassic-early Jurassic age as expressed by the Tampa Embayment (thought to be a large sag basin above an underlying rift) and the South Georgia Rift. These Phase 1 rifts underlying parts of Georgia and Florida form the southeastward extension of rifts that extend for hundreds of kilometers along the eastern margin of North America. Some of this northeastern basement fabric that is observed on regional gravity and magnetic maps may include remnant orogenic basement fabric related to the late Paleozoic Appalachian collisional event.

3. A less faulted sag basin of middle Jurassic to Cenozoic age overlies the AR and contains up to 1 km of Louann salt inferred to be of Callovian age. This Callovian salt is overlain by clastic and carbonate rocks from 7 to 9 km in thickness. Most faults and deformed strata in the sag basin are related to gravity-driven, downslope movement of Louann salt bodies.

4. Mapping of the seismic Moho beneath in the eastern GOM shows that the AR rift overlies a region of thick transitional crust with an average of 23 km of crustal thickness that likely reflects the combined effects of stretching during both rift phase 1 (Late Triassic-early Jurassic) and rift phase 2 (late Jurassic). The observed stretch factors for the crust underlying the AR varies between $\beta$=1.5 and $\beta$ =3 and are similar to other rifts studied by previous workers in other areas of the West Florida Shelf.

5. The AR rifts are inferred to be Triassic in age largely due to the known or inferred presence of the Eagle Mills Formation in surrounding Triassic-age basins including: 1) the South Georgia rift; 2) the offshore half-graben penetrated by GV-707 well (Fig. 15); and 3) several large Triassic-age rifts that were mapped by Salvador (1987) in east Texas, Arkansas, and Alabama, Mexico, and the offshore Yucatan Peninsula (Fig. 1). The crosscutting relation of the west and northwest-trending AR and Elbow rifts indicate that these west and northwest-trending rifts are younger than the northeast rift trends that are truncated (Fig. 1).

6. The Mesozoic, pre-salt stratigraphy of the syn-rift sections imaged on 2D seismic lines is best characterized by a tripartite rift stratigraphy that has been recognized by previous workers in other rift zones that includes: 1) an early-rift stage fluvial phase; 2) a mid-rift deltaic to lacustrine stage; and 3) a late-rift fluvial stage that develops as rifting wanes and transitions into an unfaulted sag phase that in the GOM is filled by thick and commonly remobilized salt deposits.

7. Several features of the internal, syn-rift stratigraphy of the AR can be identified through detailed seismic facies analysis of 2D seismic images of the internal, rift stratigraphy.

These syn-rift stratigraphic features include: 1) alluvial fan-deltas adjacent to the rift border normal fault; 2) multiple troughs/channel fill of various sizes adjacent to the border normal fault; 3) divergent reflections indicative of wedging adjacent to the rift border normal fault; 4) chaotic reflectors adjacent to the rift border normal fault representing erosional fill inferred to be conglomerate; 5) Discontinuous, prograding features in fluvial to deltaic settings emanating from either the rift border normal faults or the unfaulted but tilted side of the half-graben; and 5) chaotic, high-amplitude reflections that indicate pre-rift/basement that underlies the rift. These features are entirely based on inferences from seismic data as well control is presently not available from the syn-rift sections.

8. The alignment of the west-to-northwest trend of the AR with the parallel trend of the Elbow rift 200 km to the southeast and their crosscutting relation to older northeast trends of Phase 1 rifts underlying the West Florida Platform and the mainland of Florida indicates that the AR and Elbow rift represent an early phase of Jurassic Phase 2 extension related to the initial counterclockwise rotation of the Yucatan block. These earlier Phase 2 rifts are 200 km from the edge of the marginal rifts bounding the oceanic crust beneath the deep, central GOM and therefore these earlier Phase 2 rifts may represent a protracted middle and late Jurassic rifting stage that affected the transitional, continental crust in the eastern GOM.

9. Previous workers have identified the “Florida Lineament” or “Bahamas fracture zone” as a major, northeast-trending discontinuity in the pattern of gravity, magnetics, basement ages, and crustal thickness beneath the West Florida shelf and the mainland of Florida (Fig. 2). These previous workers presume that the Florida lineament is a major and

large-offset strike-slip feature (Fig. 2).

10. Based on the close spatial coincidence of the Florida Lineament with the AR-Elbow rift trend that I have identified, I propose that the aligned AR-Elbow rift trend provides an alternative explanation for the tectonic origin of at least the northern part of the proposed Florida lineament (Fig. 2). An apparent and relatively minor, left-lateral offset of about 20 km is observed along the AR-Elbow trend at the Tampa Embayment (Fig. 2) and may be attributed to mainly extensional of the northeastern basement trends as the result of normal faulting along the AR-Elbow rift trend.

## BIBLIOGRAPHY


Applegate, A. V., and J. M. Lloyd, 1985, Summary of Florida petroleum production and exploration, onshore and offshore through 1984: Florida Geological Survey, Information Circular, no. 101, 69 p.

Arden, D. D., 1974, Geology of the Suwannee basin interpreted from geophysical profiles, Gulf Coast Association of Geological Societies Transactions, v. 24, p. 223-230.

Bain, J., Kegel, J., and O'Reilly, C., 2019, Crustal interpretation by gravity, magnetics, and seismic data over the Gulf of Mexico, GeoGulf Transactions, v. 69, no. 1, p. 319-332.

Bally, A. W., 1987, Atlas of seismic stratigraphy: facies analysis of a depositional/seismic sequence, Shell Oil Company, AAPG Studies in Geology #27, v. 1, p. 37.

Boote, S., and Knapp, J.H., 2016, Offshore extent of Gondwanan Paleozoic strata in the southeastern United States: The Suwannee suture zone revisited, Gondwana Research, v. 40, p. 199-210.

Buffler, R. T., 1991, Early evolution of the Gulf of Mexico basin, *in* D. Goldthwaite, ed., An introduction to Central Gulf Coast geology, New Orleans Geological Society, p. 1-15.

Burg, J.P, 2018, Script to tectonics of extensional systems, ETH Zurich, 43 p.

Christenson, G., 1990, The Florida Lineament, Transactions Gulf Coast Association of Geological Societies, vol. XL, p. 99-115.

Clendenin, C. W. Jr., 2013, Insights into the mode of the South Georgia rift extension in eastern Georgia, USA, Tectonophysics, v. 608, p. 613-621.

Davison, I. and Underhill, J.R., 2012, Tectonics and sedimentation in extensional rifts: Implications for petroleum systems, *in* D. Gao, ed., Tectonics and sedimentation: Implications for petroleum systems AAPG Memoir 100, p. 15-42.

Dobson, L. M., and Buffler, R. T., 1991, Basement rocks and structure, northeast Gulf of Mexico, Gulf Coast Association of Geological Societies Transactions, v. XLI, p. 191-206.

Dobson, L. M., and Buffler, R. T., 1997, Seismic stratigraphy and geologic history of Jurassic rocks, northeastern Gulf of Mexico, AAPG Bulletin, v. 81, no. 1, p. 100-120.

Dunbar, J. A., and Sawyer, D. S., 1987, Implications of continental crust extension for plate reconstruction: An example from the Gulf of Mexico, Tectonics, v. 6, no. 6, p. 739-755.

Eddy, D. R., H. J.A. van Avendonk, G.L. Christenson, I.O. Norton, G.D. Karner, C.A. Johnson, and Snedden, J. W., 2014, Deep crustal structure of the northeastern Gulf of Mexico:

Implications for rift evolution and seafloor spreading: Journal of Geophysical Research: Solid Earth, 119, p. 6802–6822.

Ewing, T. E., and Galloway, W. E., 2019, Evolution of the northern Gulf of Mexico sedimentary basin, *in* A. Miall, ed., The sedimentary basin of the United States and Canada, Elsevier, p. 627-694.

Frederick, B. C., Blum, M. D., Lowery, C. M., and Snedden, J. W., 2016, Resolving presalt sediment source terrains and dispersal pathways for the Northern Gulf of Mexico basin, *in* C. Lowery et al. (Eds.). Mesozoic of the Gulf Rim and beyond: New progress in science and exploration of the Gulf of Mexico basin, SEPM, v. 35, p. 233-251.

Frederick, B. C., Blum, M. D., Snedden, J. W., and Fillon, R. H., 2020, Early Mesozoic synrift eagle mills formation and coeval siliciclastic sources, sink, and sediment routing, northern Gulf of Mexico basin, GSA Bulletin.

Godo, T., 2017, The Appomattox field: Norphlet Aeolian sand dune reservoirs in the deep-water Gulf of Mexico, *in* R. K. Merrill and C. A. Sternbach, eds., Giant fields of the decade 2000–2010: AAPG Memoir 113, p. 29–54.

Gohrbandt, K. H., 2002, Potential gas resources under the West Florida Shelf and slope and their development, Gulf Coast Association of Geological Societies Transactions, v. 52, p. 351-360.

Hudec, M. R., Norton, I. O., Jackson, M. P. A., and Peel, F. J., 2013, Jurassic evolution of the Gulf of Mexico salt basin, AAPG Bulletin, v. 97, No. 10, p. 1683-1710.

Hudec, M. and Norton, I. O., 2019, Upper Jurassic structure and evolution of the Yucatan and Campeche subbasins, south Gulf of Mexico, AAPG Bulletin, v. 103, No. 5, p. 1133-1151.

Hunter, I., 2014, Origin and development of the Apalachicola Basin, Unpublished master's thesis, The University of Alabama, 94 p.

Klitgord, K. D., Popenoe, P., and Schouten, H., 1984, Florida: A Jurassic transform plate boundary, Journal of geophysical research, v. 89, No. B9, p. 7753-7772.

Lin, P., 2018, Crustal structure and tectonostratigraphic evolution of the eastern Gulf of Mexico Basin, Unpublished Ph.D. dissertation, University of Houston, 141 p.

Lin, P., Bird, D. E., and Mann, P., 2019, Crustal structure of an extinct, late Jurassic-to-earliest Cretaceous spreading center and its adjacent oceanic crust in the eastern Gulf of Mexico, Marine Geophysical Research, v. 40, p. 395-418.

Liu, M., Filina, I., and Mann, P., 2019, Crustal structure of Mesozoic rifting in the northeastern Gulf of Mexico from the integration of seismic and potential field data, Interpretation, v. 7, No. 4, p. 1-12.

MacRae, G., and Watkins J.S., 1992, Evolution of the Destin Dome, offshore Florida, northeastern Gulf of Mexico, Marine and Petroleum Geology, v. 9, p. 501-509.

MacRae, G., and Watkins J.S., 1995, Early Mesozoic rift stage half-graben formation beneath the DeSoto Canyon salt basin, northeastern Gulf of Mexico: Journal of Geophysical Research: Solid Earth, v. 100, p. 17795–17812.

Mancini, E. A., Badali, M., Puckett, T. M., Parcell, W. C., and Llinas, J. C., 2001, Mesozoic carbonate petroleum systems in the northeast Gulf of Mexico, *in* R.H. Fillon, Petroleum systems of deep-water basins – Global and Gulf of Mexico experience, v. 21, p. 423-451.

Martin, R. G., 1978, Northern and eastern gulf of Mexico continental margin: stratigraphic and structural framework, *in* A. Bouma, eds., Framework, facies, and oil-trapping characteristics of the upper continental margin, AAPG, v. 7, p. 21-42.

Marzoli, A., Renne, P. R., Piccirillo, E. M., Ernesto, M., Bellieni, G., and De Min, A., 1999, Extensive 200-million-year-old continental flood basalts of the central atlantic magmatic province, Science, v. 284, No. 5414, p. 616-618.

Milici, R.C., Coleman, J. L., Rowan, E. L., Cook, T. A., Charpentier, R. R., Kirschbaum, M. A., and Schenk, C. J., 2012, Assessment of undiscovered oil and gas resources of the east coast Mesozoic basins of the Piedmont, Blue Ridge thrust belt, Atlantic Coastal Plain, and New England Provinces, 2011: U.S. Geological Survey Fact Sheet 2012-3075, p. 1-2.

Morley, C. K., 1989, Extension, detachments, and sedimentation in continental rifts (with particular reference to East Africa), Tectonics, v. 8, no. 6, p. 1175-1192.

Morley, C. K., 2009, Geometry and evolution of low-angle normal faults (LANFs) within a Cenozoic high-angle rift system, Thailand: Implications for sedimentology and the mechanisms of LANF development, Tectonics, v. 28, p. 1-30.

Nguyen, L. C. and Mann, P., 2016, Gravity and magnetic constraints on the Jurassic opening of the oceanic Gulf of Mexico and the location and tectonic history of the Western Main transform fault along the eastern continental margin of Mexico, Interpretation, v. 4, no. 1, p. 23-33.

Neumaier, M. and Mouli-Castillo, J., 2014, Basin analysis and petroleum systems modeling of the Lokichar Basin (Kenya), Search and Discovery Article #10676, Adapted from oral presentation at AAPG International Conference & Exhibition, Istanbul, Turkey, 47 p.

Olsen, P. E., 1990, Tectonic, climatic, and biotic modulation of lacustrine ecosystems – examples from Newark Supergroup of eastern North America, *in*. B. Katz, editor, Lacustrine basin exploration: Case studies and modern analogs, AAPG Memoir, v. 50, p. 209-224.

Osmundsen, P. T., and Peron-Pinvidic, G., 2018, Crustal-scale fault interaction at rifted margins and the formation of domain-bounding breakaway complexes: Insights from offshore Norway, Tectonics, v. 37, p. 935-964.

Pashin, J. C., Guohai, J., and Hills, D. J., 2016, Mesozoic structure and petroleum systems in the de soto canyon salt basin in the mobile, Pensacola, destin dome, and viosca knoll areas of the mafla shelf, *in* C. Lowery, eds., Mesozoic of the gulf rim and beyond: new progress in science and exploration of the Gulf of Mexico basin, SEPM, v. 35, p. 416-449.

Pindell, J. L., 1985, Alleghenian reconstruction and subsequent evolution of the Gulf of Mexico, Bahamas, and Proto-Caribbean, Tectonics, v. 4, no. 1, p. 1-39.

Post, P. J., and Coleman, J. L. Jr., 2015, Mesozoic rift basins of the U.S. Central Atlantic offshore: Comparison with onshore basins, analysis, and potential petroleum prospectivity, *in* P. Post, eds., Petroleum Systems in "Rift" Basins, SEPM, v. 34, p. 1-93.

Ratcliffe, N. M., Burton, W. C., D'Angelo, R. M., and Costair, J. K., 1986, Low-angle extensional faulting, reactivated mylonites, and seismic reflection geometry of the Newark basin margin in eastern Pennsylvania, Geology, v. 14, p. 766-770.

Raymond, D. E., 1989, Eagle Mills Formation of the Alabama Coastal Plain, *in* C. Copeland, eds., Upper Cretaceous and Tertiary lithostratigraphy and biostratigraphy of west-central Alabama, Alabama Geological Society, Guidebook, no. 26, p. 75-92.

Salvador, A., 1987, Late Triassic-Jurassic paleogeography and origin of Gulf of Mexico Basin: American Association of Petroleum Geologists Bulletin, v. 71, p. 419-451.

Salvador, A., 1991, Origin and development of the Gulf of Mexico basin, *in* A. Salvador, The Gulf of Mexico basin, v. J, p. 389-444.

Sandwell, D. T. and Smith, W. H. F., 2009, Global marine gravity from retracked Geosat and ERS-1 altimetry: ridge segmentation versus spreading rate, Journal of geophysical research, v. 114, p. 1-18.

Sawyer, D.S., Buffler, R.T., and Pilger, R.H., Jr., 1991, The crust under the Gulf of Mexico basin, *in* Salvador, A., The Gulf of Mexico Basin, v. J, p. 53–72.

Schultz, A. P., 1988, Hydrocarbon potential of eastern Mesozoic basins, United States Geological Survey, Open-file report 88-299, p. 1-17.

Snedden, J. W., and Galloway, W. E., 2019, The Gulf of Mexico sedimentary basin: depositional evolution and petroleum applications, Cambridge University Press, 326 p.

Steier, A. and Mann, P., 2019, Late Mesozoic gravity sliding and Oxfordian hydrocarbon reservoir potential of the northern Yucatan margin, Marine and Petroleum Geology, v. 103, p. 681-701.

White, N., and McKenzie, D., 1988, Formation of the "steer's head" geometry of sedimentary basins by differential stretching of the crust and mantle, Geology, v. 16, p. 250-253.

Wilson, K., 2011, The origin and development of the Tampa Embayment: Implications for the tectonic evolution of the eastern Gulf of Mexico, Unpublished master's thesis, The University of Alabama, 63 p.

Withjack, M. O., Schische, R. W., Olsen, P.E., 2002, Rift-basin structure and its influence on sedimentary systems, *in* R. Renault, eds., Sedimentation in Continental Rifts, SEPM Special Publication, No. 73, p. 57-81.

Withjack, M. O., Schische, R. W., Malinconico, M.L., and Olsen, P.E., 2013, Rift-basin development: Lessons from the Triassic-Jurassic Newark Basin of eastern North America, *in* W. Mohriak, eds., Conjugate divergent margins, Geological Society of London, Special Publications, v. 369, p. 301-321.

Xiao, H., and Suppe, J., 1992, Origin of rollover, AAPG Bulletin, v. 76, No. 4, p. 509-529.

Yallup, C., The pre-salt of southern Mexico: Is there potential for oil?, *in* Exploration Insights Halliburton Landmark, p. 18-23.